Individual-based model of population dynamics in a sea urchin of the Kerguelen Plateau (Southern Ocean), Abatus cordatus, under changing environmental conditions

Margot Arnould-Pétré, Charlène Guillaumot, Bruno Danis, Jean-Pierre Féral, Thomas Saucède

Version of Record: https://www.sciencedirect.com/science/article/pii/S030438002030418X
Manuscript_f20659540bea3bcd336db43977514d0a

Individual-based model of population dynamics in a sea urchin of the Kerguelen Plateau (Southern Ocean), *Abatus cordatus*, under changing environmental conditions

Authors: Arnould-Pétré Margot [a,*], Guillaumot Charlène [a,b], Danis Bruno [b], Féral Jean-Pierre [c], Saucède Thomas [a]

[a] UMR 6282 Biogéosciences, Univ. Bourgogne Franche-Comté, CNRS, EPHE, 6 bd Gabriel F-21000 Dijon, France

[b] Laboratoire de Biologie Marine, Université Libre de Bruxelles, Avenue F.D.Roosevelt, 50. CP 160/15. 1050 Bruxelles, Belgium

[c] Aix Marseille Université/CNRS/IRD/UAPV, IMBE-Institut Méditerranéen de Biologie et d'Ecologie marine et continentale, UMR 7263, Station Marine d'Endoume, Chemin de la Batterie des Lions, 13007 Marseille, France

* Corresponding author. Email address: m.arnould-petre@nhm.ac.uk (M. Arnould-Pétré)

Individual-based model of population dynamics in a sea urchin of the Kerguelen Plateau (Southern Ocean), *Abatus cordatus*, under changing environmental conditions

Keywords: ecological modelling; Kerguelen; climate change; model sensitivity; endemic echinoderm; Dynamic Energy Budget; Individual-based model

Highlights:

- A DEB-IBM model was built for the sea urchin *Abatus cordatus* using literature data
- Monthly environmental conditions are available at the reference station
- The model was implemented in contrasting food and temperature conditions
- The sea urchin population structure and dynamics were evaluated in time
- A sensitivity analysis was performed to test for model robustness

Abstract

The Kerguelen Islands are part of the French Southern Territories, located at the limit of the Indian and Southern oceans. They are highly impacted by climate change, and coastal marine areas are particularly at risk. Assessing the responses of species and populations to environmental change is challenging in such areas for which ecological modelling can constitute a helpful approach. In the present work, a DEB-IBM model (Dynamic Energy Budget – Individual-Based Model) was generated to simulate and predict population dynamics in an endemic and common benthic species of shallow marine habitats of the Kerguelen Islands, the sea urchin *Abatus cordatus*. The model relies on a dynamic energy budget model (DEB) developed at the individual level. Upscaled to an individual-based population model (IBM), it then enables to model population dynamics through time as a result of individual physiological responses to environmental variations. The model was successfully built for a reference site to simulate the response of populations to variations in food resources and temperature. Then, it was implemented to model population dynamics at other sites and for the different IPCC climate change scenarios RCP 2.6 and 8.5.

Under present-day conditions, models predict a more determinant effect of food resources on population densities, and on juvenile densities in particular, relative to temperature. In contrast, simulations predict a sharp decline in population densities under conditions of IPCC scenarios RCP 2.6 and RCP 8.5 with a determinant effect of water warming leading to the extinction of most vulnerable populations after a 30-year simulation time due to high mortality levels associated with peaks of high temperatures. Such a dynamic model is here applied for the first time to a Southern Ocean benthic and brooding species and offers interesting prospects for Antarctic and sub-Antarctic biodiversity research. It could constitute a useful tool to support conservation studies in these remote regions where access and bio-monitoring represent challenging issues.

1. Introduction

The Kerguelen Islands are part of the French Southern Territories (Terres australes françaises - Taf), located at the limit of the Indian and Southern oceans, in the sub-Antarctic area. The region is highly impacted by climate change, and coastal marine ecosystems and habitats are particularly at risk given that species have long adapted to cold and stable conditions (Waller et al. 2017, Gutt et al. 2018, Convey & Peck 2019). Coastal marine species of the Kerguelen Islands are threatened by temperature and seasonality shifts, which are expected to intensify in a near future (Turner et al. 2014, IPCC 5th report). Future predictions of the Intergovernmental Panel on Climate Change (IPCC 5th report) are provided as possible Representative Concentration Pathways (RCP) scenarios of climate change and can be used to infer the potential response of ecosystems to future environmental conditions. However, the insufficient spatial and time resolutions of such models constitute serious limitations to assessing the effects of future environmental changes on sub-Antarctic species (Murphy & Hofmann 2012, Constable et al. 2014).

The echinoid *Abatus cordatus (Verrill 1876)* is endemic to the Kerguelen oceanic plateau and common in coastal benthic habitats of the Kerguelen Islands. It is reported in the northern Kerguelen plateau, and around Heard and Kerguelen islands but most records are from shallow, coastal areas of the Kerguelen Islands where dense populations are commonly observed (Agassiz 1881, De Ridder et al. 1992, Mespoulhé 1992, Poulin 1996, David et al. 2005, Hibberd & Moore 2009, Guillaumot et al. 2016, Guillaumot et al. 2018a,b). This makes the species particularly at risk considering the synergetic effects of the multiple factors (temperature variations, significant shifts in coastal currents, sedimentation rates and phytoplanktonic blooms) affecting coastal marine communities at high latitudes

(Waller et al. 2017, Stenni et al. 2017, Gutt et al. 2018). The species' endemicity can be partly related to low dispersal capabilities, which is a consequence of a particular life trait: *A. cordatus* broods its young in incubating pouches located on the aboral side of the test, and has a direct development with no larval stage and no metamorphosis. The low dispersal capacity of *A. cordatus* likely increases its vulnerability to environmental changes (Ledoux et al. 2012).

Benthic fauna of sub-Antarctic regions remains under-studied compared to pelagic species (Améziane et al. 2011, Xavier et al. 2016). Ecological niche models can represent relevant tools to study the consequences of environmental changes on the biology of these benthic organisms and on their population dynamics. Correlative niche models were used to predict the distribution of suitable areas for *A. cordatus* on the Kerguelen plateau (Guillaumot et al. 2018a,b). However, supplementary data and analyses are still needed to depict and understand the species' response to environmental changes.

In the present work, a mechanistic modelling approach using a Dynamic Energy Budget - Individual-Based Model (DEB-IBM) was used to analyse the biological response of *A. cordatus* to various environmental conditions. An individual mechanistic model (DEB) was first built using experimental and literature data (Guillaumot 2019). A DEB model aims to represent the physiological development of an organism, from the embryo to its death based on energetic fluxes and allows considering the metabolic state of the individual at any given moment of its life cycle. It relies on biological principles and first laws of thermodynamics to recreate the metabolic development as a function of two environmental parameters, food resources and temperature (Kooijman 2010).

The DEB model was then upscaled to the population level (IBM), wherein it was implemented as iterative mathematical calculations of each organism's individual development in the population. The IBM relies on the simulation of individuals as autonomous entities forming a complex population within a dynamic system (Railsback and Grimm 2019). The DEB-IBM is used to analyse population dynamics emerging from the development and the physiological traits of individuals as a function of environmental forcing variables (i.e. food resources and temperature). The DEB-IBM can then be used to simulate population dynamics under different environmental scenarios, enabling a better quantification of the vulnerability of populations to changing environmental conditions.

Modelling population dynamics using a DEB-IBM model for a sub-Antarctic and brooding invertebrate brings a feature so far unseen in other published DEB models. The main objectives of the study were to develop a DEB-IBM model for *A. cordatus* (1) to simulate population structure and dynamics at different sites under both current

environmental conditions and future IPCC climate scenarios RCP 2.6 and RCP 8.5, and (2) to assess the feasibility of such a model for organisms in a region where low data availability and resolution may limit model building and validation. The current resolution and accuracy of future climate scenarios in sub-Antarctic areas do not allow building precise and reliable predictions for the future but they were used here as a proof of concept to test population responses to various, conceivable conditions. Sensitivity analyses were performed to test the robustness, potential and relevance of models (Grimm & Berger 2016) considering data availability. Simulations performed for various temperature conditions and food resource availabilities, if validated, may constitute a promising tool to address conservation issues.

2. Methods

2.1. Study area

The DEB-IBM population model was generated in the geographic and environmental context of the Kerguelen Islands (Fig. 1) using data of the study site of Anse du Halage, a fieldwork station that has regularly been investigated through several biological studies since the 1980s (Magniez 1980, Schatt & Féral 1991, Mespoulhé 1992, Poulin 1995, Poulin & Féral 1998, Ledoux et al. 2012). The Kerguelen Islands show jagged coastlines and numerous islets and fjords that provide a large variety of habitats to the marine benthic fauna. The nature of the seafloor varies from rocky to sandy and muddy shores. The predominance of the giant kelp *Macrocystis pyrifera* is a main feature of the Kerguelen as this engineer and key species plays a decisive role in the protection and structuring of benthic shallow habitats in many places of the archipelago (Lang 1967, 1971, Arnaud 1974, Féral et al. 2019).

Located in the Morbihan Bay, a 700 km^2 semi-enclosed shallow embayment (50m depth on average) of the Kerguelen Islands, Anse du Halage is situated at the bottom of a small and shallow (2m depth) cove dominated by fine to medium sands (Magniez 1979, Poulin 1996) (Fig. 1). The tidal range is comprised between 0.4 and 2.1m, so that the area can exceptionally be uncovered at the lowest tides (Schatt and Féral 1991, Mespoulhé 1992). Sea surface temperature varies between 1 and 2°C in winter (September) to 7 to 8°C in summer (March), with sporadic peaks of +11°C in some places for certain years (Schatt and Féral 1991, Féral et al. 2019). Salinity varies between 31.89 and 33.57 (Arnaud 1974).

Temperature data used in the model were collected in the framework of the Proteker programme (French Polar Institute n°1044) (Féral et al. 2019) and accessed online (IPEV programme n°1044, http://www.proteker.net/-

Thermorecorders-.html?lang=en accessed on 08/05/2019). They were recorded from 2012 to 2018 at three sites used in the model (Fig. 1): Ile Longue (for the model at Anse du Halage), Ile Haute, an island in the North-Western corner of the Morbihan Bay, and Port Couvreux, a coastal site outside the Morbihan Bay, in the Gulf of the Baleiniers on the Northern coast of the archipelago (Fig. A.1).

The organic matter deposited on the seabed varies with seasonal phytoplankton blooms and remineralization by bacteriae (Delille et al. 1979). The sediment organic content and phytoplanktonic blooms are particularly important at Anse du Halage, with average values of 4.5% of organic carbon content. The sediment organic carbon (OC) content was measured monthly as a percentage of sediment dry weight by Delille & Bouvy (1989).

Environmental data time-series are available at a monthly timestep. The model was scaled on a single square metre patch, supposing no connectivity between neighbour locations, as no data on horizontal nor vertical water movements and matter fluxes were available.

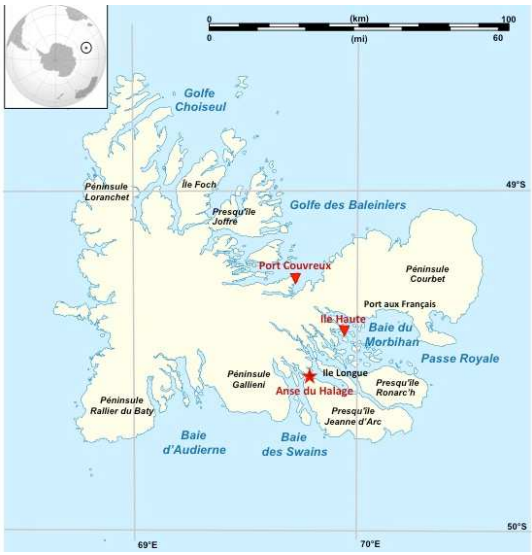

Figure 1. Location of the studied sites in the Kerguelen Islands, calibration site (Anse du Halage, red star) and projection sites (Ile Haute and Port Couvreux, red triangles).

2.2 Study species

Abatus cordatus (Fig. 2) is a shallow deposit-feeder and sediment swallower, living at 5°C average, full or half buried into soft sediments (De Ridder and Lawrence 1982). It is distributed all around the Kerguelen Islands, but

population densities are highly variable depending on depth, substrate nature and exposure to the open sea. Distributed from the intertidal area to the deep shelf over 500m depth, populations highest densities are found in very shallow (0-2m depth) and sheltered areas with soft bottoms of fine to medium sand (Poulin 1996). In shallow areas, observed density vary from less than 5 individuals/m^2 (in the Fjord des Portes Noires, Poulin & Féral 1995) to 10 ind./m^2 (at Port-aux-Français, Mespoulhé 1992), 130 ind./m^2 (Ile Haute, Mespoulhé 1992, Poulin 1996), 168 ind./m^2 (Port Couvreux, Poulin 1996) and up to 280 ind./m^2 (Anse du Halage, Magniez 1980, Poulin 1996). Juveniles are commonly found sheltered in between holdfasts of the giant kelp *Macrocystis pyrifera* bordering with sandy shallow areas.

The species is relatively resistant to low salinities locally induced by freshwater run-off from the main island (Guille & Lasserre 1979). It is tolerant to temperature variations, particularly marked in shallow areas, but temperature tolerance does not exceed +12°C (personal observations). The maximum size ever observed is 4.9 cm in length (Mespoulhé 1992). Lifespan is assumed to be around six years old (Mespoulhé 1992), although it cannot be excluded that some individuals may grow older. Identified predators are gastropods, crustaceans and seagulls (Poulin & Féral 1995, Poulin 1996) from which the specimens are hidden when burrowing into the sediment (Magniez 1979, Poulin & Féral 1995).

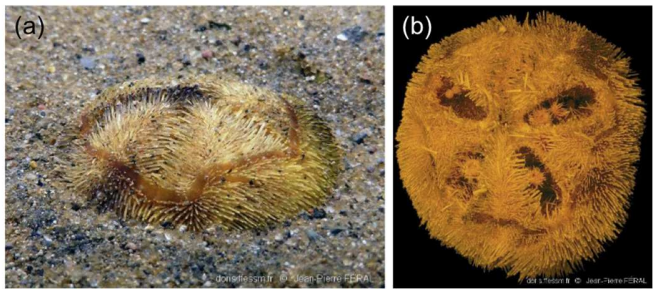

Figure 2. Specimens of *Abatus cordatus*. (a) Aboral view of a specimen half buried in sand, (b) Aboral view of a female showing the brood pouches with juveniles inside. © Féral J.P.

Sexual reproduction in *A. cordatus* occurs every year, with all mature females producing eggs (Magniez 1983) and incubating their young in their four brood pouches located on the aboral side of the test (Fig. 2b). After brooding, juveniles exit the pouches and start their autonomous development on the seabed, in the vicinity of their mother (Magniez 1983, Schatt 1985). Reproduction time can greatly differ between sites: generally extending from March to

May (as in Anse du Halage and Ile Haute), reproduction can also occur from June to August (Ile Suhm), from December to February (Port Matha) or from August to November (Port Couvreux) (Poulin 1996). Females usually spawn once a year (Poulin 1996). Brooding and burrowing behaviours imply a relative sedentary lifestyle and can explain a part of the species endemicity, with dense populations scattered all around the archipelago and only a few older individuals that may be found isolated from core populations (Mespoulhé 1992, Poulin & Féral 1995).

2.3 DEB modelling

2.3.1. Principles

DEB theory defines individuals as dynamic systems and provides a mathematical framework for modelling organisms' life cycle. It describes physiological processes using four primary state variables —reserve, structure, reproduction buffer and maturity— directly linked to mass and energy flows and influenced by two forcing variables, temperature and food availability (Fig. 3, Kooijman 2010, Jusup et al. 2017). Based on feeding, growth and reproduction processes, DEB models predict the metabolic and development states of organisms through time (Sousa et al. 2008, Kooijman 2010). Metabolic processes are linked to shape and size of the organism, represented by the structural volume and the structural area. Structural volume is related to maintenance processes, while structural area is closely linked to food ingestion and assimilation processes and controls the amount of energy arriving into the reserve compartment E (Fig. 3A, van der Meer 2006).

The energy contained in the reserve compartment is allocated to organism maintenance ('somatic' and 'maturity' maintenances, priority processes that condition the organism's survival), to growth (increase of structural volume V), and to the increase of complexity (E_H) or reproduction buffer (E_R) (Fig. 3A) according to the kappa-rule (Kooijman 2010). The complexity is represented as the maturity level. The amount of energy accumulated into this compartment triggers metabolic switches such as the transition (i.e. ability to feed, to reproduce) between life stages, defined in DEB theory (namely embryo, juvenile and adult life stages) (Kooijman 2010).

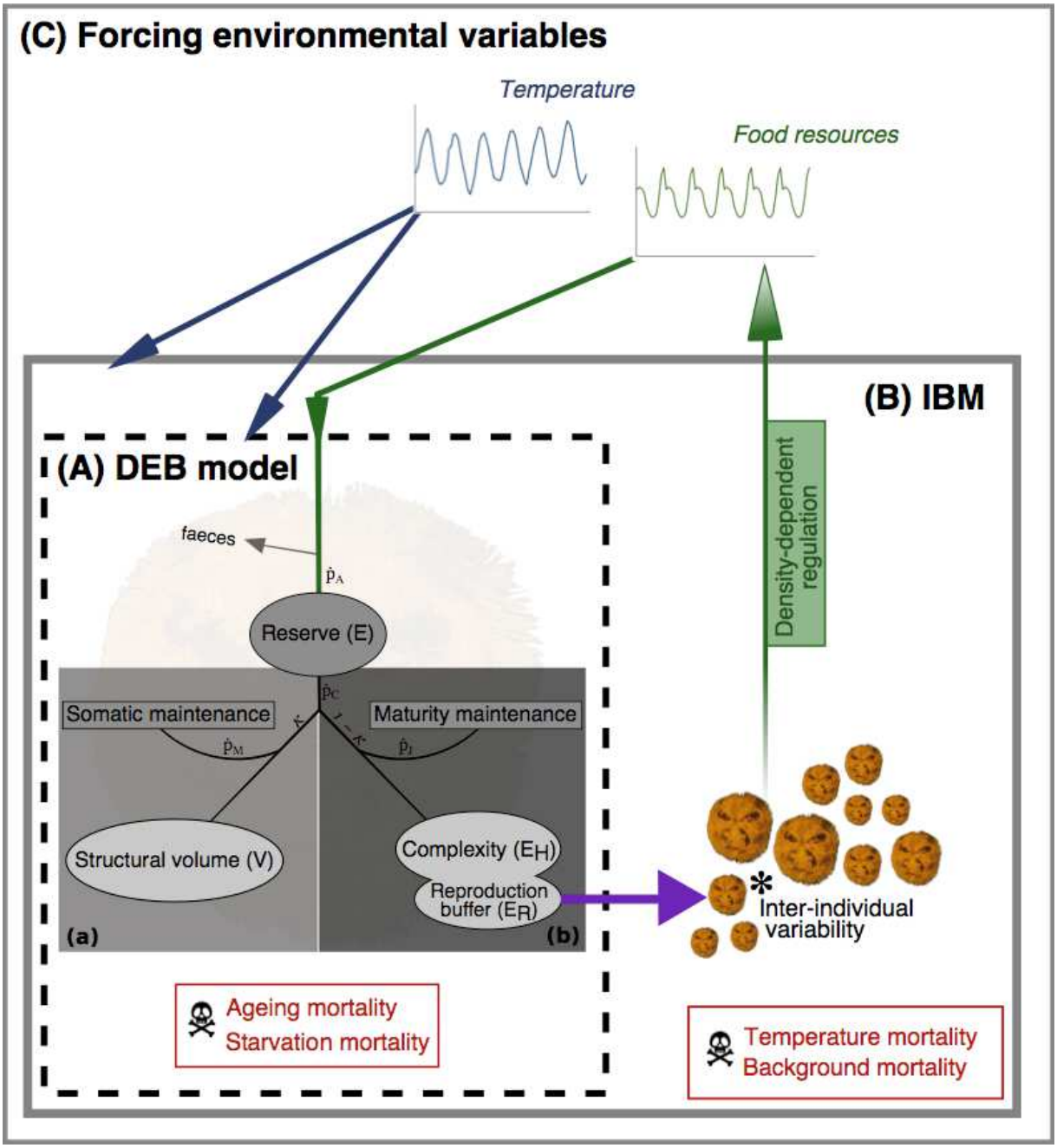

180

181 **Figure 3.** Schematic representation of the DEB-IBM (Dynamic Energy Budget - Individual-Based Model).
182 Individuals (A) undergo development through the DEB model and reproduce (purple arrow). Altogether and with a
183 slight inter-individual variability in DEB parameters (*), they form the population of the IBM (B) which undergoes
184 population-specific processes (temperature and background mortalities) at the scale of a simple square metre patch at
185 the reference site (C). The IBM population is embedded within this specific environment, whose environmental

conditions (temperature and food resources) affect individual and population dynamics. Additionally, the population influences the resources availability following a density-dependence regulation.

2.3.2. Application of DEB model to A. cordatus

Parameter estimation. An individual mechanistic DEB model was developed for *A. cordatus* (Guillaumot 2019). Estimated DEB parameters are reported in Table 1. The DEB model considers a larval growth accelerated compared to the adult stage (Schatt 1985), so-called 'abj' type model. The model was constructed using data from the literature (Table 2). The goodness of fit of the DEB model to the data was evaluated by calculating the Mean Relative Error (MRE) of each dataset, which is the sum of the absolute differences between observed and expected values, divided by the expected values. MRE values are contained in the interval [0, infinity). The MRE is considered to be a reference method to assess DEB modelling performance (Lika et al. 2011b), for which the closer to 0, the better model predictions match the data.

Table 1. Parameters estimated for the DEB model developed for *Abatus cordatus*. Values are given for the reference temperature of 20°C. The MRE of the model is 0.121.

Parameter	**Symbol**	**Value**	**Unit**
Basic DEB parameters			
Volume of specific somatic maintenance[1]	$[\dot{p}M]$	13.84	$J.d^{-1}.cm^{-3}$
Somatic maintenance rate coefficient[1]	$\dot{k}M$	5.10^{-3}	d^{-1}
Fraction of energy allocated to somatic maintenance and growth[1]	κ	0.78	-
Volume-specific cost of structure[1]	[EG]	2395	$J.cm^{-3}$
Energy of maturity at birth[1]	$[E_H^b]$	0.5693	$J.cm^{-3}$
Energy of maturity at metamorphosis[1]	$[E_H^j]$	8.325	$J.cm^{-3}$
Energy of maturity at puberty[1]	$[E_H^p]$	1638	$J.cm^{-3}$
Arrhenius temperature[3]	TA	9000	K
DEB compound parameters			
Energy conductance[1]	$\dot{v}$	0.02722	$cm.d^{-1}$
Maturity maintenance rate coefficient[3]	$\dot{k}J$	0.002	d^{-1}
Shape coefficient[2]	δ	0.6718	-
Maximum structural length [1]	L_m	2.93	cm
Acceleration factor[1]	sM	2.397	-

Reproduction parameters			
Yield of structure on reserve[1] Contribution of reserve to weight[1]	yVE w	0.865 0.647	#mol.mol^{-1} -
Ageing parameters			
Weibull ageing acceleration[1] Gompertz stress coefficient[3]	ḧa sG	5.02.10^{-6} 0.0001	d^{-2} -

[1] Estimated using the covariation method (Lika et al. 2011a, 2011b, Marques et al. 2018)

[2] Calculated from data for initial value and then estimated with the covariation method

[3] Fixed, guessed value

Table 2. Zero and uni-variate data used for the estimation of the DEB model parameters. All values are given at a measured temperature of 5°C. MRE: Mean Relative Error. Plots related to uni-variate data can be found in Appendix B.

Variable	**Symbol**	**Obs.**	**Prediction**	**Unit**	**MRE**	**Reference**
Zero-variate data						
Age at metamorphosis[1]	aj	142	143	d	0.0072	Schatt (1985)
Age at puberty[2]	ap	1098	1018	d	0.0731	Mespoulhé (1992)
Life span	am	2190	2190	d	5.10^{-8}	Mespoulhé (1992)
Length at metamorphosis	Lj	0.276	0.324	cm	0.1738	Schatt (1985)
Length at puberty	Lp	1.9	1.824	cm	0.0399	Mespoulhé (1992)
Maximal observed length (at 6 years old)	L6	4.2	3.65	cm	0.1321	Mespoulhé (1992)
Ultimate maximal length	Li	8	9.507	cm	0.1883	guessed
Wet weight of the egg	Ww0	1.78.10^{-3}	1.59.10^{-3}	g	0.1081	Schatt (1985)
Wet weight at metamorphosis	Wwj	1.03.10^{-2}	1.70.10^{-2}	g	0.6482	Schatt (1985)
Wet weight at puberty	Wwp	2.9	3.03	g	0.0448	Féral and Magniez (1988)
Wet weight at 6 years old	Ww6	25	24.18	g	0.0328	Féral and Magniez (1988)
Gonado-somatic index[3]	GSI	0.07	0.078	-	0.1194	Magniez (1983)

Variable	**Symbol**	**Obs. /Prediction**	**Unit**	**MRE**	**Reference**
Uni-variate data					
Time since birth vs. length	tL	See Appendix B	d // cm	0.2259	Schatt and Féral (1996)
Egg diameter vs. egg wet weight	LW_egg		cm // g	0.1262	Mespoulhé (1992)
Length vs. Wet weight adult	LW		cm // g	0.3248	Féral and Magniez (1988)
Length vs. O2 consumption	LJO		cm // µL/h	0.2872	Féral and Magniez (1988)

[1] moment at which the juveniles leave the brooding pouch of the mother

[2] moment at which the sea urchin is able to reproduce

[3] maximum gonad index for an animal of the maximum size, gonad index as gonad weight/total wet weight.

Maturation and development. Embryos of *A. cordatus* have a direct development in brood pouches of females (Magniez 1983, Schatt 1985). They start feeding inside pouches after 142 days of incubation (i.e. 5 months) and leave the pouches as fully developed sea urchins after 8.5 months (Schatt 1985). According to DEB theory, individuals are considered embryos until they can feed (Kooijman 2010). Before the fifth month, feeding inside the maternal pouches is not clearly attested, but feeding through epidermal uptake of Dissolved Organic Matter (DOM) is considered as the possible mechanism (Schatt & Féral 1996). At each growth step, energy is supplied to the reserve by the ingested food (Fig. 3A, $\dot{p}_A$) and then leaves the reserve compartment to be directed to growth, maturation or reproduction compartments through the mobilisation flux (Fig. 3A, $\dot{p}_C$). This is performed following the kappa-rule: a κ fraction is directed towards the structure (growth compartment and somatic maintenance, Fig. 3A(a)), and the remaining $1 - \kappa$ fraction towards complexity (maturation, reproduction compartments and maturity maintenance, Fig. 3A(b)).

During the juvenile stage, the individual does not supply energy into reproduction, but accumulates energy in its maturity compartment E_H until reaching the 'puberty' threshold that, according to DEB theory, defines the moment when the organism is mature enough to reproduce (Kooijman 2010). After reaching this threshold, at around 2.5 to 3 years old (Schatt 1985, Mespoulhé 1992), the organism can allocate energy into the reproduction buffer E_R for gamete production (Fig. 3A). The structural volume increases continuously along the individual's life, from birth to death, supplied in energy left from what has not been allocated to priority maintenance costs $\dot{p}_M$ and $\dot{p}_J$.

Starvation mortality. Magniez (1983) observed that the gonadal index continues to decrease slightly for around two months after reproduction. He hypothesized that it was related to the season: as the reproduction period finishes at the start of winter, food resources decrease and energy investment into reproductive organs is momentary diverted towards the maintenance of somatic elements. This was demonstrated in the other sea urchin species *Strongylocentrotus purpuratus* (Lawrence et al. 1966) and *Arbacia lixula* (Fenaux et al. 1975) confronted to starvation. In the model, when scaled reserve e (reserve relative to reserve capacity, no dimension) falls below the scaled structural length l (length relative to maximum length, no dimension), it is assumed that the individual is

confronted to starvation: the kappa-rule is then altered as energy is entirely redirected to the somatic maintenance and all other fluxes (growth, reproduction or maturation) are set to 0. When $e < 0$, the organism does not have enough energy to allocate the amount necessary for survival (somatic maintenance costs) and dies. See section "7.Submodels/Starvation" in Appendix G for further details and implemented equations.

Ageing mortality. Death probability by senescence was calculated in the model using the ageing sub-model, a simulation of damages induced by lethal compounds such as free radical or other reactive oxygen species (ROS), following the DEB theory for ageing (Kooijman 2010).

The density of damage inducing compounds in the body increases as the reserve compartment is fuelled with energy that is allocated through the entire organism. It influences the hazard mortality rate $\dot{h}$, which is a function of the damage accumulated in the body and simulates the vulnerability of the individual to damages, such as the risk of dying from illness increases with age. In the model, the hazard mortality rate $\dot{h}$ is supplemented by a stochastic parameter (Martin et al. 2010) to control the ageing mortality rate. See section "7.Submodels/Ageing" in Appendix G for further details and implemented equations.

2.4 Individual-based modelling for the population

2.4.1 Principles

The individual DEB model is used to simulate each individual as an entity of the individual-based population model (IBM). An IBM represents the individual components (individuals of *A. cordatus*) of an environmental system (Anse du Halage) and their behaviours, enabling to feature each individual as an autonomous entity and looking at results at the scale of the whole population (DeAngelis & Mooij 2005, Grimm & Railsback 2005, Railsback & Grimm 2019). In our model, each individual do not have any direct interaction nor adaptive behaviour towards their environment nor the other members of the population. They follow a continuous development governed by metabolic fluxes (DEB model) that are influenced by environmental conditions (temperature and food resources) along their entire life. Each individual is a component of the modelled population, which is itself affected by population death rate and density-dependent processes.

The IBM was built with the software Netlogo version 6.0.4 (Wilensky 1999), using the DEB-IBM model developed by Martin et al. (2010) for the species *Daphnia magna*. The NetLogo code is available at

http://modelingcommons.org/browse/one_model/6201. It contains the script to run the model, the input files of monthly food resources and temperatures for the three stations and a detailed description of the model following the ODD protocol from Grimm et al. (2010) and the associated list of variables present in the code. This detailed ODD was also included in Appendix G.

2.4.2 Application of IBM model to A. cordatus

Model structure. The model includes two types of entities: the individuals and the environment. Individuals are divided into 4 types of sub-agents, depending on their life stage and sex: embryos, juveniles, adult males and adult females. The values of four primary state variables are attributed to each individual (scaled reserve U_E, volumetric structural length L, scaled maturity U_H and scaled reproduction buffer U_R). The level of energy contained in the scaled maturity U_H thresholds the life stages. These four variables are 'scaled', meaning here that the energy dimension has been removed by dividing with the surface-area-specific maximum assimilation rate $\{\dot{p}_{Am}\}$ (in $J.L^{-2}.t^{-1}$), based on DEB theory (Kooijman 2010).

Simulations were run with a monthly timestep for calculation, in regard to the slow growth of the species and the available data (an analysis of the effect of the timestep on the core individual model was conducted, cf. Appendix C). At each timestep, food and temperature conditions are first input into the model, state variable values of each individual are calculated in order to assess whether new maturity thresholds are reached or whether energy is sufficient for survival, growth or reproduction. The population state is reassessed at the end of each month. Spatially, population structure and density are simulated on a patch of one square metre at each site and individuals do not leave the patch during their entire life.

Initialisation. The initial population density value was set to 120 ind./m^2 and this figure was split into classes of equal densities of 20 individuals of different age-classes, between 0 and 5 years old, in order to stabilize the initialisation between the different replicates. An initial run is realised to capture the values of the four state variables that characterize the individual of each age class (at October 2012 temperatures and f=1), in order to initiate the model (Appendix H).

The first decade of the simulation period was always considered as the initialisation phase and was removed from the analysis, the model showing important outliers (in individual metabolism and population structure) during these first ten years.

Inter-individuals variability. Each individual is characterized by similar energetic performances estimated by the DEB estimation (Table 1). Five DEB parameters were divided by a *scatter-multiplier* parameter that was generated in order to create inter-individual variability. These five DEB parameters were selected because they are associated to the four state variables that characterize the individuals and are not null at the time the individual is initiated into the model (following Martin et al. 2010): (1) maturity level at birth (U_H^b, d.cm^2), that is the amount of energy accumulated in the maturity compartment needed to reach the *juvenile* stage; (2) maturity level at *puberty* (U_H^p, d.cm^2), the amount of energy accumulated into the maturity compartment to reach the adult stage; (3) energy investment ratio (g, no dimension), the cost of the added volume relative to the maximum potentially available energy for growth and maintenance; (4) the initial energy reserve at *birth* (U_E, d.cm^2); and (5) the initial structural length (L, cm).

The *scatter-multiplier* is the exponential of a random number from a normal distribution of mean 0 and standard deviation *cv* (0.1 by default, can be set by the user in the interface of the model). The value is therefore small enough to not affect tremendously the initial variable and generate trade-off between parameters. It is applied as soon as the individual is created in the system.

Reproduction. Sex-ratios (ratio males/females) in the studied populations are slightly contrasting between localities, from 0.94 (Ile Haute) to 0.99 (Anse du Halage) and 1.04 (Port Couvreux) (Poulin 1996). The average ratio of 0.99 was chosen in the model. By approximation, it was considered that only females undergo physiological changes during the reproduction process, males being only used as a component of the total population.

To this date, few monitoring studies have been performed on *A. cordatus* reproduction. Magniez (1983) is the only one who studied the Gonado Somatic Index (GSI), that is the proportion of ash-free gonads dry weight over the ash-free body dry weight, therefore directly linked to the accumulation of energy into the reproduction buffer. According

to Magniez (1983), reproduction can occur if the GSI reaches at least 0.07%. This condition was used in our model to control the ability of the female to reproduce when time comes.

The gonadosomatic index GSI was only attributed to females and was estimated for each month, with this equation (Kooijman 2010, section 4.10, eq. 4.89):

$$GSI = \frac{time\_of\_accumulation * \dot{k}_M * g}{f^3 * (f + \kappa * g * y_{VE})} * \left((1 - \kappa) * f^3 - \frac{\dot{k}_J * U_H^p}{Lm^2 * s_M^3}\right)$$, where the time of accumulation is the number of days spent since the end of the reproduction period, $\dot{k}_M$ is the somatic maintenance rate coefficient (in d^{-1}), g the energy investment ratio (no dimension), f the scaled functional response (no dimension), κ the fraction of energy directed towards structure, y_{VE} the parameter for the yield of structure on reserve (mol/mol), that is the number of moles of structure that can be produced with one mole of reserve, $1 - \kappa$ the fraction of energy directed towards complexity, $\dot{k}_J$ the maturity maintenance rate coefficient (in d^{-1}), U_H^p the scaled energy in the complexity compartment at puberty ($d.cm^2$), L_m the maximum structural length (cm), and s_M the acceleration factor (no dimension).

The reproduction period is constant from March to May for the individuals at Anse du Halage, and they only spawn once a year (Magniez 1983, Schatt & Féral 1996, Poulin 1996). After each monthly step, the model checks the GSI value for each female. If the GSI reaches the 0.07% threshold at the onset of the period (March), reproduction is triggered for this considered female.

According to the literature, when reproducing, females invest around 52% of their reproductive organs' energy into reproduction (Magniez 1983). This energy is released during the three months when spawning occurs. That is, the GSI of the female will decrease by 52% of its initial value over the 3 months period (so a decrease of one third of 52% per month, with $\partial GSI = (GSI_{start} - 0.52 * GSI_{start}) / 3$, where GSI_{start} is the level of gonadal index at the onset of reproduction). In parallel, the usual ∂U_R (change in energy density in the reproduction buffer outside of the reproduction period, no unit) is set to 0 for the three months, while U_R (energy density in the reproduction buffer) is forced to decrease in a similar fashion to the GSI: $\partial_2 U_R = (U_{R\_start} - 0.52 * U_{R\_start}) / 3$, with U_{R_start} being the reproduction buffer at the start of the period.

Reproduction induces the introduction of 27 embryos in average in the system (Magniez 1983), added proportionally along the three months (9 per month).

Background mortality. No specific adult mortality rates are mentioned in the literature, as no cause have been defined precisely. Background population mortality annual rates were estimated based on size frequency distribution provided by Mespoulhé (1992), and using the formula from Ebert (2013) $N(t) = N_0 * e^{-M*t}$ with N(t) the population size at time t, N_0 the initial population size, M the mortality rate and t the time (in months). Two yearly mortality rates were defined: one for juveniles (41%) and one for adults (24%).

A percentage of embryos mortality in the pouches was calculated based on data from Poulin (1996), determining an egg survival of 65%. This mortality is associated to the fact that when the first juveniles start leaving the maternal pouches at the beginning of January, they push aside the protecting spikes of the pouch, and eggs remaining in the brood are no longer protected and die (Magniez 1980).

Mortality induced by temperatures. As no precise information is available to accurately describe *A. cordatus* temperature tolerance, three different types of sensitivity were designed to cover different hypothesis (Fig. D.2). Based on experimental results obtained in the Kerguelen Islands (personal observation), mortality gradient due to temperature was applied to the population for temperatures comprised between 8 and 12°C. Over 12°C, all individuals are considered to die in the model, as none survived in the experiment. (1) A 'vulnerable' type was defined with population death rates of 25%, 35% and 45% when the sea urchins are exposed to temperatures respectively reaching 8, 9.5 and 11°C during two consecutive months. (2) The 'resistant' type was defined with a mortality rate 15% lower than the vulnerable one for the same temperature thresholds (e.g. 10% instead of 25% population mortality at +8°C), for similar exposure duration (i.e. two months). (3) The 'intermediate' type is similar to the 'resistant' type but individuals are considered to die after one month of exposure to each temperature instead of two (Fig. D.2).

Density-dependent regulation. Population density autoregulates through competition for food resources. This procedure relies on the monitoring of population density in relation to the carrying capacity and allows to stabilize the model. The model calculates the current population density and quantifies the competition effect on food availability depending on how far from the carrying capacity (K) the population density (P) is, and updates food availability in accordance.

It is considered that at each timestep, a certain amount of food is available in the environment (f_{env}) but according to population size, competition for food (FC, quantified food competition) is present and influences effective food availability (f_{eff}), with $f_{eff} = f_{env} + FC$, following Goedegebuure et al. (2018). f_{eff} and f_{env} are contained between 0 and 1. FC is calculated with the following equations:

If $P < 1.9 * K$, then $FC = (1- f_{env}) . (1 - \frac{P}{2.K-P})$

If $P \geq 1.9 * K$, then $FC = (1- f_{env}) . (1 - \frac{P}{K/10})$

FC is positive if $P < K$, and f_{eff} tends to its maximal value 1 with a decreasing population size, as FC becomes very low and tends to $1- f_{env}$. When $P > K$, FC turns negative and makes f_{eff} decrease with the minimal value reached at $P = 2K$.

Two equations are used because if $P = 2K$, the first formula gives an error due to a division by 0, and if $P > 2K$, then the formula gives the untrue result of less competition with a bigger population (hence the use of 1.9 as a pivot value). Competition is only effective if food availability is less than the maximum (hence the use of '$1 - f_{env}$' in the equation).

2.5. Summary of model parameterization and sensitivity analysis

The model was constructed following the ecological and physiological observations available in the literature for *A. cordatus*. These observations are summarised in the following table (Table 3). Once these elements added, the ageing submodel and the carrying capacity parameters, for which no *in situ* observations are defined, were calibrated until obtaining a model stable in time, over several centuries.

The sensitivity of the model to different parameters was tested. This sensitivity analysis also served as a first form of validation in the absence of wider means of validation. Initial population number, inter-individuals variation coefficient, juvenile and adult background mortalities, number of eggs produced per female during a reproduction event, and egg survival rate were each applied variations of -30%, -20%, -10%, +10%, +20% and +30% (Table 3). The influence of changes in these parameter values was assessed on the average population density (ind/m^2), the average juvenile/adult ratio, the average physical length, the average reserve energy and the average structural length variation over the period of 200 years. For each analysis, models were replicated 100 times. A model was considered to 'crash' when the population is not stable and collapses entirely before the end of the simulation period. The

405 proportion of crashes relates to the number of crashes counted for 100 simulations (i.e., for 15 crashes and 100
406 simulations, the proportion is 15/(100+15)~13%). Due to computing time limitations, the analysis was stopped when
407 reaching a proportion higher than 66% of crashes (indicated by a black cross in Appendix E).
408
409 The model sensitivity to the GSI threshold assumption was tested with the upper and lower values of the GSI
410 calculated at the onset of reproduction in Magniez (1983). The minimum value did not impact the model at all, but
411 the higher threshold value prevented most of the females from reproducing (results not presented).
412
413 **Table 3.** List of parameters integrated in the individual and population models. Descriptions and values. The source
414 reference that justifies the choice of the parameterization is provided in the 'reference' column. The last column
415 synthetises which parameters where modified to performed a sensitivity analysis, whose results are presented in
416 Appendix E.

Parameters	Model parameterization	Reference	Sensitivity analysis
Individuals			
Time of development until birth	8 months	254 days (Schatt 1985)	MRE DEB model
Time of development until puberty	Threshold by U_H^b value	2.5 to 3 years old (Schatt 1985, Mespoulhé 1992)	MRE DEB model
Starvation	e < 1	Kooijman (2010)	Not tested
Ageing	Probability depending on accumulated cell damages, constrained by stochasticity	Damage probability: following Martin et al. (2010) and Kooijman (2010) rules for ageing Stochasticity: calibrated at the end of model construction until reaching model stability	Not tested, calibrated parameter
Population			
Initial population density	120 ind./m^2	Rounded from literature (Guille and Lasserre 1979, Magniez 1980, Mespoulhé 1992, Poulin 1996)	-30 to +30% variation tested
Initial population structure	5 age-classes of 20 individuals	Follow average population structure observed by Mespoulhé (1992)	Not tested

Variation coefficient (cv) from the inter-individual variability	0.1	Follow IBM parameterization of Martin et al. (2010) study	-30 to +30% variation tested
Ratio females/males	50/50	Sex-ratio: 0.99 (Poulin 1996)	Not tested
Initial GSI	0.03%	Magniez (1983)	Not tested
GSI threshold for reproduction	0.07%	Magniez (1983)	Tested with the upper (0.116) and lower (0.028) values of the GSI calculated at the onset of reproduction in Magniez (1983)
Reproduction period	3 months once a year	Magniez (1983), Schatt & Féral (1996), Poulin (1996)	Not tested
Energy investment into reproduction	52% of the reproductive energy at the onset of the period	Magniez (1983)	Not tested
Number of eggs	27 eggs per adult female	Magniez (1983), Schatt (1985)	-30 to +30% variation tested
Eggs survival to juvenile stage (birth)	65%	Poulin (1996)	-30 to +30% variation tested
Yearly background mortality rates	41% of juveniles 24% of adults	Equation provided in Ebert et al. (2013), implemented with population data from Mespoulhé (1992)	-30 to +30% variation tested
Mortality induced by temperature tolerance	Three sensitivity scenarios	Designed from experimental results	Not tested
Carrying capacity	200 ind./m^2	Calibrated at the end of model construction until reaching model stability, no information available in the literature	Not tested, calibrated parameter

417

418

419 *2.6. Forcing environmental variables*

420

421 *2.6.1. Temperature*

In the frame of DEB theory, temperature influences metabolic rates following the Arrhenius function which defines the range of temperatures that affect enzyme performance, considering that metabolic rates are controlled by enzymes that are set inactive beyond an optimal temperature tolerance (Kooijman 2010, Thomas & Bacher 2018). The Arrhenius response is characterized by five parameters that describe the species tolerance range: the Arrhenius temperature T_A, the temperature at the upper and lower limits of the species tolerance range T_H and T_L respectively, and the Arrhenius temperature beyond upper and lower limits of the tolerance range T_{AH} and T_{AL} respectively.

In our study, the available information is not sufficient to define the complete relationship between temperature and metabolic performances, and the temperature correction factor (*TC*) is only calculated using one of the five Arrhenius parameter T_A (in K), following the equation $\boldsymbol{\tau}(T) = \boldsymbol{\tau} * \exp(T_A/T_{ref} - T_A/T)$ with $\boldsymbol{\tau}$ a given metabolic rate, T_{ref} the reference temperature (293K ≈ 20°C), T the environmental temperature (in Kelvin) and $\exp((T_A/T_{ref} - T_A/T)$ being the temperature correction factor *TC*. The correction is applied to the metabolic rates $\dot{v}$, $\dot{k}_M$, $\dot{k}_J$, $\ddot{h}_a$ (Table 1).

Temperatures recorded since 1993 at Port aux Français, another site in the Gulf of Morbihan, show a clear 6-year cycle of increasing and decreasing temperatures (Appendix A). The [2012-2018] temperature dataset selected as input forcing variable in the model therefore constitutes an interesting proxy of temperature conditions at Anse du Halage which includes a complete overview of the environmental variability at the station. However, it is important to take this choice into consideration during interpretation of results, as it needs to be differentiated from a cycle that would be inherent to the biology of the species.

2.6.2. Food resources

In DEB theory, the energy is supplied to the reserve of the organism through ingestion proportional to food availability, represented in the model by a functional response *f* (from 0 to 1). Food assimilation ($\dot{p}_A$, Fig. 3A) is proportional to the surface of the structure of each individual and contributes to the filling of the reserve compartment *E* (Fig. 3A). The functional response *f* was calibrated using the values of organic carbon (OC) content in sediment as a percentage of dry weight of sediment at the station Anse du Halage at the end of each month, available in Delille & Bouvy (1989). The maximum value of 1 for *f* corresponds here to the maximum value of organic carbon content that was found (6.94%) and a *f* minimum of 0 corresponds to 0% OC.

2.7 Model projection

2.7.1. Present-day conditions at Anse du Halage

To assess the influence of varying environmental conditions on model outputs, after being constructed for the site Anse du Halage, the model was implemented in two other sites, Ile Haute and Port Couvreux, where *A. cordatus* is reported in high densities (Poulin 1996) (Fig. 1). The implementation to these two other stations was done with contrasting temperatures (from the Proteker programme, as previously explained in 2.1). Food conditions at these two sites are not available and were estimated at the end of the summer to be 50% to 30% of the organic carbon values measured at Anse du Halage according to the comparative study of Delille et al. (1979). These rates were applied to yearlong conditions (Fig. A.2). Models were launched for a period of 200 years.

2.7.2. Future conditions

Two future scenarios predicting environmental conditions for 2100 were used, based on the IPCC scenario RCP 2.6 and 8.5 (respectively optimistic and pessimistic scenarios, IPCC 5th report), accessed at https://www.esrl.noaa.gov/psd/ipcc/ocn/ (in August 2019). Coarse IPCC predictions (1°x1° resolution) of chlorophyll a concentration were used to roughly evaluate potential changes of food availability on the east coast of the Kerguelen Island in future conditions. Scenario RCP 2.6 shows an average decrease of 10% of current food resources availability, while scenario RCP 8.5 shows an average decrease of 20% (Fig. D.3). As for temperature, we defined RCP 2.6 with a linear increase of +1.1°C and +1.7°C for RCP 8.5. Models were launched for a period of 30 years.

3. Results

3.1 The individual-based model

Variations in energy allocated to the reserve and the maturation buffer are the main controls of individual development. Monthly variations (∂U_E and ∂U_R, ∂X here stands for $\frac{dX}{dt}$) were simulated over one year under present-day environmental conditions (Fig. 4). Energy in the reserve (Fig. 4a) shows variations between -2.5 and 8 on

478 average (no unit), with maximum range values reaching -5.8 and 13.7. This shows a relative constant energy density
479 inside the reserve throughout the year with, however, a noticeable increase from October to December and a sharp
480 decrease from December to January (Fig. 4a). According to DEB theory (Kooijman 2010), the more energy is stored
481 inside the reserve (through food assimilation), the more it can be distributed to other compartments, and the more
482 energy can be assimilated into the reserve anew. Availability of food resources for *A. cordatus* is the highest in
483 December (f = 1) (Fig A.2), it is assimilated and stored as energy into the reserve. Based on the energy available in
484 the reserve at the end of December, energy is supplied in January to other compartments (such as the reproduction
485 buffer, Fig. 4b and growth, Fig. Fa), while the individual ingests the food available to replenish its reserve anew. As
486 food availability decreases in January (f = 0.748), the reserve loses energy (Fig. 4a) because the individual cannot
487 assimilate as much energy as the amount transferred to other compartments.
488
489 The energy density entering the reproduction buffer (Fig. 4b) of mature females varies between 0 and 4.9 on average
490 in the course of the year, with a maximum of 10.7. The rate of energy input increases at an average pace of +1.1%
491 per month from October to the onset of the reproduction period in March, when it decreases and remains null until
492 the end of the spawning period in June. Then, energy starts accumulating again until the next reproduction period.
493 During the three months of the spawning period, from March to May, no energy is allocated from the reserve to the
494 reproduction buffer and the energy stored in this buffer is progressively delivered to gametes. Only females that are
495 mature in March undergo reproduction and deliver the energy contained in the reproductive buffer to the gametes.
496 Females that become mature during the reproduction period undergo a normal increase of the energy in the
497 reproduction buffer, which explains the small increasing trend observed during the March-May period (Fig. 4b).
498
499

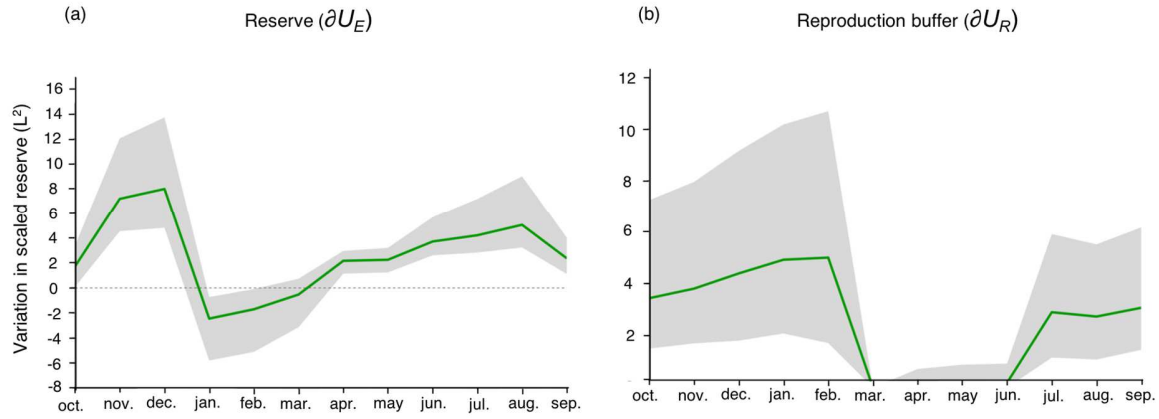

Figure 4. Simulation of the variation of energy allocated to the reserve (a) and the reproduction buffer (b) compartments over one year. Males were not considered in the model when simulating reproduction processes, and thus results presented here only take females into consideration. Average results for all mature females, in 100 model simulations are presented by the green line. The grey area corresponds to the variation range (variation induced by differences between individuals: age, size, energy allocation) between all females among the 120 individuals that initiate the model. The variation in energy allocated is the change in a scaled variable X: ∂X here stands for $\frac{dX}{dt}$ (for an explanation of the term "scaled" here, see section 2.4.2).

3.2 The population model

3.2.1. Modelled population dynamics at the calibration site

Based on the individual model, population dynamics were simulated over a time period of 30 years, showing a constant population density comprised between 120 and 220 individuals per square metre. Overall, the population structure remains constant through time but with well-marked yearly variations, mainly in juvenile density (Fig. 5). Juveniles indeed represent around 83% of the total population density and show important yearly variations due to (1) important seasonal reproductive outputs causing a surge in population density, (2) strong mortality rates causing gradual decreases in the population, (3) the transfer of the large juvenile cohort to the adult population after around 3 years, and (4) the influence of inter-individual competition for food limiting population densities and even causing its decrease. In contrast, the adult population is much more stable relative to the juvenile one, with lower density values (around 40 individuals per square metre). Both juvenile and adult population fluctuations follow a general 6-year pattern displayed over the 30 years of simulations (rectangle, Fig. 5). This pattern is linked to temperature cycles

over the same time span and includes two sharp decline in population density over a 6-year cycle ('T' symbol, Fig. 5), which corresponds to high temperatures rising above +8°C during two consecutive months and causing mortality rates of 10% of the entire population.

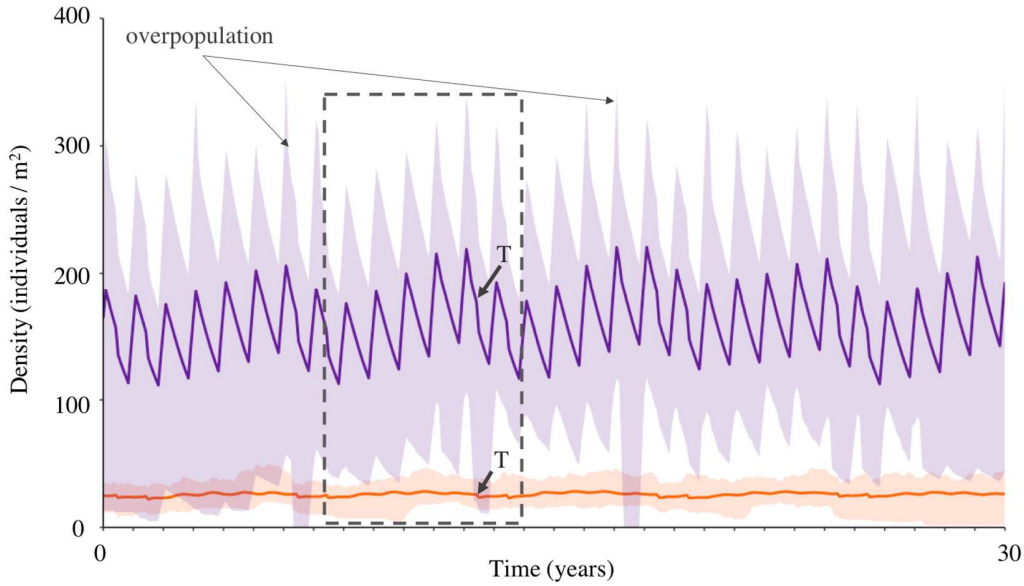

Figure 5. Modelled population structure and density under present-day environmental conditions: monthly values of juvenile density (purple) and adult density (orange) over 30 years (for 100 simulations). Bold lines: mean density value. Shaded areas: variation range for the 100 simulations. 'T' symbol: sharp decrease in population density due to temperature-induced mortality. Dashed-line rectangle: 6-year cycle in population dynamics (this 6-year pattern is due to the input temperature data and not to a biological cycle inherent to the population).

3.2.2 Sensitivity analysis

Different parameter settings for the model initiation may result in very diverging outputs (Appendix E). It also influences model stability, and population collapse in particular. Overall, the initial number of individuals and the level of the inter-individual variation coefficient are parameters that have little influence on model stability and low proportion of population crashes may result. In addition, model outputs do not differ significantly between simulations. Increase in juvenile and adult mortality levels will also have little influence on model outputs but

decreasing mortality levels will induce a population burst followed by a strong competition for food and a consequent population collapse.

Among all the parameters set at the model initialisation, egg number and egg survival are the most important determining model stability, as they directly control juvenile density. High juvenile densities (induced by a low background juvenile mortality and a high number of eggs and egg survival) always result in fast population collapses as a result of high competition for food between individuals. As population density increases, the amount of food available for each individual decreases and individuals start starving to death. In contrast, a reduction in the number of juveniles causes a reduction in the average population density due to a strong mortality rate of juveniles. It does not imply model instability and the proportion of modelled population crashes is always lower than 15%. The reduction of population density also strongly influences the average amount of energy available for each individual: the more energy is available, the more individuals can grow in structural length.

3.2.3. Projections of the population dynamics model to other sites

The dynamic population model built at Anse du Halage was implemented (Appendix G) for the two sites of Ile Haute (inside the Morbihan Bay) and Port Couvreux (outside the Morbihan Bay). Both models were simulated twice with initial estimates of 50% and 30% of food availability (f) compared to Anse du Halage (f_H). Temperature inputs were based on local temperature variations recorded at the two sites. Model outputs predict lower population densities at both sites compared to Anse du Halage and interestingly, similar ratios between juveniles and adults (Table 4). These results are consistent with density values found in the literature, which give between 100 and 136 individuals/m^2 at Ile Haute and 50 to 168 ind./m^2 at Port Couvreux (Mespoulhé 1992, Poulin 1996). The different observed density values reported in publications for Port Couvreux may be due to contrasting conditions that locally prevail among the three small embayments of that locality (Poulin 1996). This has recently been confirmed by our personal observations in the field (Saucède 2020). Model outputs suggest a strong influence of food availability on population densities controlled by inter-individual competition for food. Accordingly, simulations predict a drop in density values at Port Couvreux when food resources decrease at 30% of f_H, while density values are relatively stable at Ile Haute in comparison (Table 4a). This mainly affects juvenile densities and results in a lower population ratio (Table 4b).

565 Temperatures recorded at the two sites inside the Morbihan Bay (Anse du Halage and Ile Haute) are close to each
566 other and slightly higher than outside the Bay at Port Couvreux (Fig. A.1). Contrasting results were therefore
567 expected between Port Couvreux and the two other sites. On the contrary, temperatures may not be contrasting
568 enough between sites to affect population structure and density. Confidence intervals overlap between all sites for
569 values of both population density and juveniles-adults ratio (Table 4).
570
571 **Table 4.** Modelled population densities (a) and juveniles over adults ratio (b) at the calibration (Anse du Halage)
572 and projection (Ile Haute and Port Couvreux) sites. Average and standard deviation values are given for 100 model
573 replicates and 200 years of simulation. f_H: time series of *f* value at Anse du Halage (Delille & Bouvy 1989).

(a)	Anse du Halage	Ile Haute	Port Couvreux
f_H , T°Halage	182.6 ± 49	-	-
50% of f_H, T°site	-	137.6 ± 40	137.4 ± 41
30% of f_H, T°site	-	123.2 ± 38	91.8 ± 44

574

(b)	Anse du Halage	Ile Haute	Port Couvreux
f_H , T°Halage	6.53 ± 3.12	-	-
50% of f_H, T°site	-	6.31 ± 4.40	6.32 ± 4.31
30% of f_H, T°site	-	6.04 ± 4.31	3.87 ± 2.61

575
576
577 *3.2.4. Population dynamics under future predictions of climate change*
578 Population structure and density were simulated and implemented for scenarios of temperature and food
579 resources changes based on IPCC scenarios RCP 2.6 and 8.5, and for populations of 'resistant', 'intermediate' and
580 'vulnerable' organisms (Fig. 6). Population dynamics are all predicted to be affected by both scenarios (Fig. 6d, 6g)

581 with overall population densities predicted to be four to seven times lower than current population predictions.
582 Population structures are also predicted to be affected by a lower contribution of juveniles to overall population
583 densities. The respective effects of temperature (Fig. 6b) and resource availability (Fig. 6c) were simulated
584 independently. Under temperature change only (Fig. 6b), model predictions are close to model outputs in which both
585 variables are combined (Fig. 6g), with a strong decrease in average population density compared to present-day
586 conditions (Fig. 6a). The effect of changes in resources availability only (Fig. 6c) is less marked, with population
587 densities showing a close pattern to present-day models (Fig. 6a).

588 Models therefore predict a stronger effect of temperature changes on populations, with population densities of
589 ‘vulnerable' organisms predicted as very low (less than one tenth of present-day densities on average). Populations of
590 'vulnerable’ organisms are even predicted to go extinct in only 30 years of simulation (Fig. 6f, 6i). Populations of
591 organisms with 'intermediate' sensitivity (Fig. 6e, 6h) are more resilient and withstand over 30 years of simulation in
592 some cases, but they collapse at the end of the period under IPCC scenario RCP 8.5. Overall densities are very low
593 (around 20 or less individuals per square metre on average).

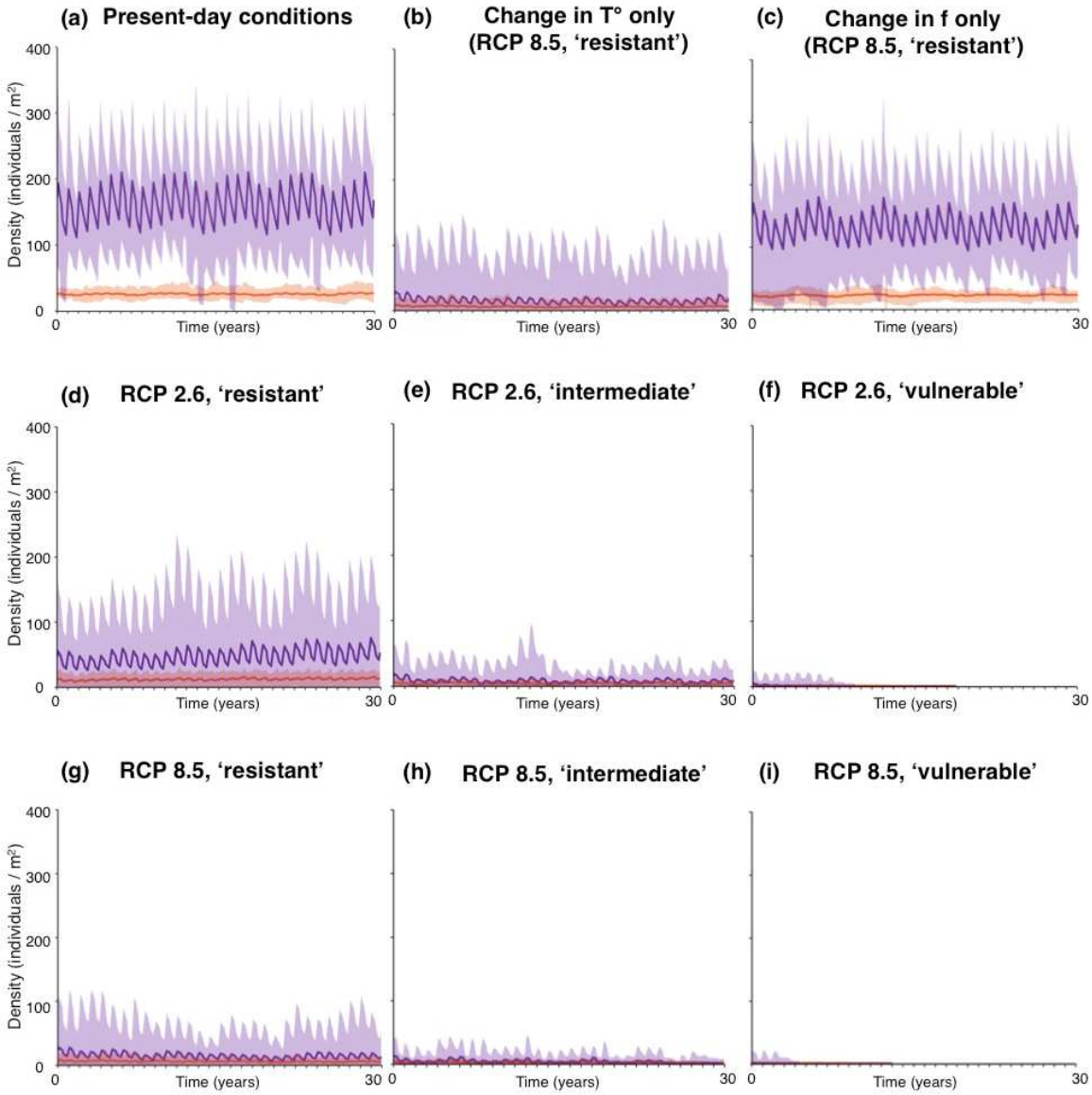

Figure 6. Model predictions under IPCC scenarios RCP 2.6 and RCP 8.5 of environmental change (for 100 simulations). Purple: adult population, orange: juvenile population. Coloured bold lines show mean values for 100 simulations. Shaded areas are simulation variation ranges. (a) Population model under present-day conditions, (b) model under IPCC scenario RCP 8.5 of T° change only (+1.7°C compared to present) and for resistant organisms; (c) model under IPCC scenario RCP 8.5 of *f* change only (-20% compared to present) and for resistant organisms; (d) model under IPCC scenario RCP 2.6 of T° and *f* changes (-10% of *f* and +1.1°C compared to present) and for 'resistant' organisms; (e) model under IPCC scenario RCP 2.6 of T° and *f* changes and for 'intermediate' organisms; (f) model under IPCC scenario RCP 2.6 of T° and *f* changes and for 'vulnerable' organisms; (g) model under IPCC

603 scenario RCP 8.5 of T° and *f* changes and for 'resistant' organisms; (h) model under IPCC scenario RCP 8.5 of T°
604 and *f* changes and for 'intermediate' organisms; (i) model under IPCC scenario RCP 8.5 of T° and *f* changes and for
605 'vulnerable' organisms.
606
607 *3.3. Population mortality under present-day and future predictions*
608 Under present-day conditions (Fig. 7b), background mortality and ageing are the main causes that affect
609 population mortality each year (respectively between 65 to 90% and 5.8 to 9%). High temperatures and starvation
610 have sporadic effects on mortality. High mortality due to high temperatures only happened in [2016-2017] and
611 [2017-2018] and starvation contributes at the highest to 10% of overall mortality, depending on the year.
612 Over the course of a year (Fig. 7a), background mortality and ageing affect the population every month, while
613 high temperatures (over 8°C) cause the death of half of the population in March and April. Starvation is responsible
614 for the death of a weak proportion of the population in November and December only (austral summer), in link with
615 the competition for food resources of the increasing population during this productive and warm period.
616 Under both future scenarios (Fig. 7e, 7f), mortality levels are low compared to present-day model (Fig. 7b),
617 which is mostly due to small predicted population densities. Background and ageing mortalities are therefore very
618 low. Starvation is not a cause of mortality anymore, while high temperatures cause mortality of individuals before
619 they may starve to death. When comparing between model predictions under scenario RCP 8.5 for changes in food
620 availability only (Fig. 7c), temperature change only (Fig. 7d), and the combined variables (Fig. 7f), temperature
621 clearly appears as the main cause of mortality, at the same level as background mortality.

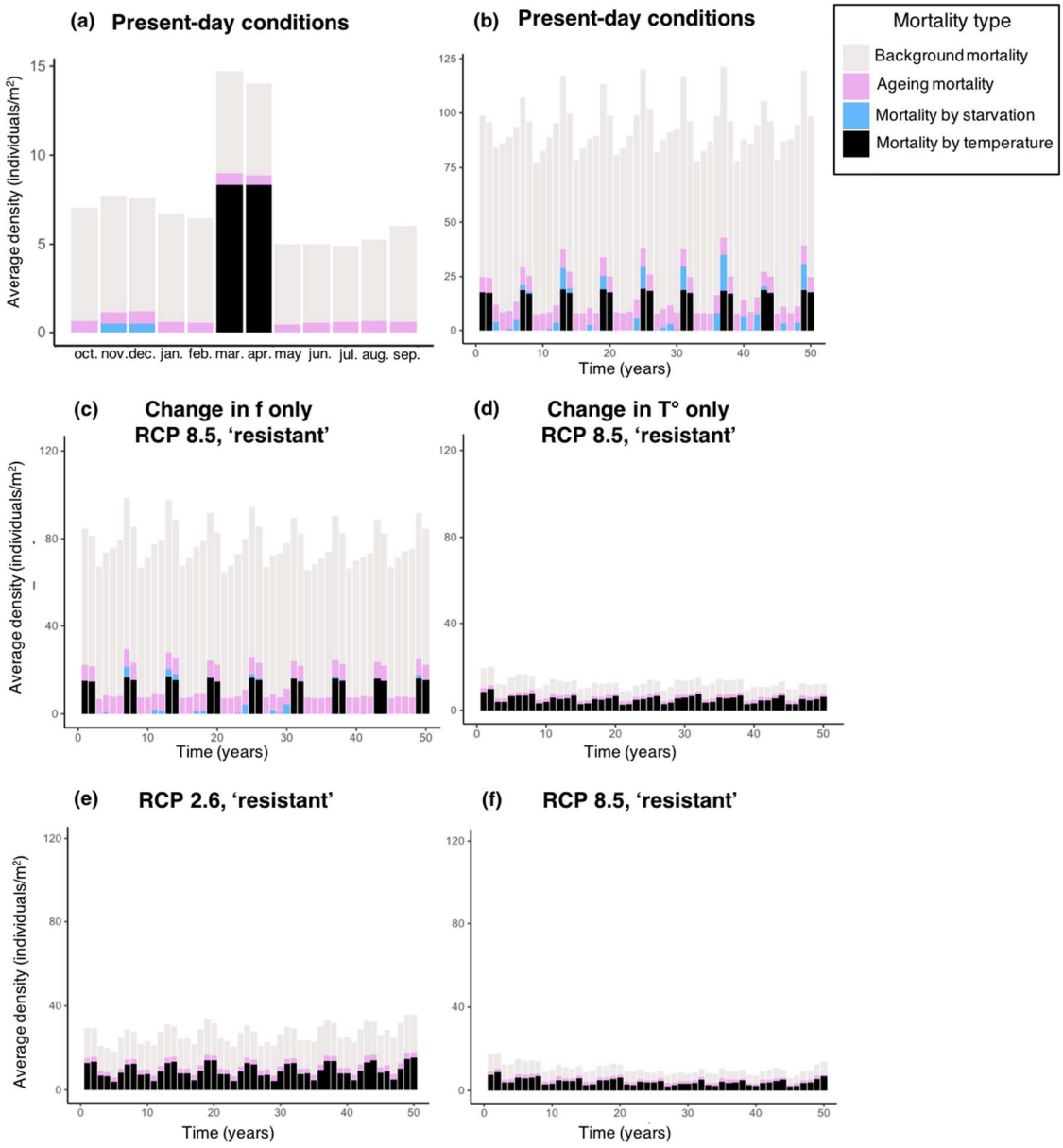

622

623 **Figure 7.** Mortality simulations (in individuals/m^2) per month (7a) and year (7b-f) under present-day (7a-b) and
624 future (7c-f) predictions of the two IPCC scenarios (for 100 model simulations). (a) Model under present-day
625 conditions for 12 months (year #7 [2016-2017] was chosen as an example); (b) Model under present-day conditions
626 for 50 years of simulations; (c) Simulated mortality under scenario RCP 8.5 for resistant organisms and predicted
627 changes in food availability only (*f*=-20% compared to present); (d) Simulated mortality under scenario RCP 8.5 for
628 resistant organisms and predicted changes in temperature only (+1.7°C compared to present); (e) Simulated mortality
629 under scenario RCP 2.6 for resistant organisms and predicted changes in both food availability and temperature (food

reduction of -10%, T° increase of +1.1°C); (f) Simulated mortality under scenario RCP 8.5 for resistant organisms and predicted changes in food availability and temperature (food reduction of -20%, T° increase of +1.7°C).

4. Discussion

4.1. Potential and limitations of the DEB-IBM approach

In the present work, a DEB-IBM model was built for *A. cordatus* based on our current knowledge of this vulnerable, endemic species of the Kerguelen plateau. On-site monitoring and experiments on species tolerance to changing environmental conditions remains challenging issues in the Kerguelen Islands, and in the Southern Ocean in general. Difficulties are owed to the sensitivity of specimens (Magniez 1983, Schatt 1985, Mespoulhé 1992) and the inherent ecological characteristics. Models can constitute a powerful tool for Antarctic research as they can provide additional support to experimental knowledge and infer the impact of broad-scale climate change on populations. The potential of the present mechanistic modelling approach resides in its capacity to model the physiology of organisms as a response to environmental factors. Using DEB models for the representation of individual components within the IBM enables to upscale a dynamic model to an entire population (Railsback & Grimm 2019) as a function of two changing abiotic factors: temperature and food resources. Applying such a model to a sub-Antarctic, benthic, and brooding species is challenging, and had never been performed so far. The present work shows the feasibility and relevance of the DEB-IBM approach to study Southern Ocean species like *A. cordatus*.

Relevant results were obtained both at the individual and populations levels. First, simulations showed the characteristic annual evolution of energy dynamics in the organism (Fig. 4, Appendix F) and second, population structure and density dynamics were modelled over an extended period of time decoupling juvenile and adult populations (Table 4, Fig. 6, Fig. 7). Projections to other sites also show the potential application of the model to other areas for which environmental data are available. Future models give an insight and add some clues to assess the potential impact of climate change and predict the biotic response of populations. Models however still need some improvements including complementary data on species ecophysiology. The model was also shown to be sensitive to mortality rates and some parameters (egg number and egg survival) settings while some population characteristics (initial population densities and inter-individual variability) have little effects (Appendix E).

4.2. Limitations to the DEB-individual model

The dynamic population model built in this work uses outputs from the DEB model developed for *A. cordatus* (Guillaumot 2019), which allows to represent as faithfully as possible the physiological dynamics of individuals during their entire life cycle. The goodness of fit of the DEB model shows that estimated parameters accurately described observed data. However, collecting additional data at the different stages of the organism's life cycle and under different conditions of temperature and food availability would contribute to improving further model accuracy and parameter predictions. In particular, data on environmental settings and species ecophysiology are still needed to improve the accuracy and relevance of the following parameters.

4.2.1. The Arrhenius function and the optimal temperature range

In DEB theory, the Arrhenius function determines the optimal temperature range of the organism's metabolism as a response to enzymatic tolerance (Kooijman 2010, Thomas & Bacher 2018). In the present work, calculation of the Arrhenius function relies on fragmental datasets. The ascending part of the Arrhenius curve that is, the temperature range in which faster metabolic rates are determined by higher temperatures was estimated, but values are still missing for the descending slope (i.e. the temperature range beyond the optimal temperatures in which the metabolic rates slow down with higher temperatures) (Kooijman 2010). The present model assumes that higher temperatures favour more suitable conditions with no limit (Appendix F), which has to be corrected arbitrarily using our personal field and experimental observations on the echinoid ecology (Fig. D.2). Further experiments should help improve the calculation of the Arrhenius function. They would consist in measurements of respiratory rates as a function of temperature variations (e.g. Uthicke et al. 2014) and will enable more accurate simulations of *A. cordatus*' ecophysiology and the direct effect of temperature on the organism's metabolism, a prerequisite to better model population mortality.

4.2.2. Age, size, and growth estimates

Most parameters used in the DEB model were taken from the literature and experimental studies, except for some of them that were assumed based on physiological traits of counterparts. In particular, organisms' maximum age, growth rate and size are not sufficiently known due to difficulties in setting up long-term experiments in the

686 Kerguelen Islands. The relationship between echinoid growth, size and shape cannot be assessed based on growth
687 lines measurement because there is no linear relationship between echinoid size and age (Ebert 1975) and because
688 resorption may occur during periods of starvation (Brockington et al. 2001, Ingels et al. 2012). The most reliable
689 method would consist in monitoring organisms' growth through time using tagging methods (Ebert 2013). However,
690 such an approach is time-consuming and challenging as even small measurement errors may have a significant effect
691 on results (Ebert 2013) and no experimental data are available so far.

692 Former studies (Mespoulhé 1992) showed that after 4 to 5 years, specimens of *A. cordatus* only slowly increase
693 in size and echinoids' test tend to become distorted, a common feature in large spatangoid echinoids in which test
694 plates tend to overlap while body size does not increase anymore (Mespoulhé 1992). However, this slow growth rate
695 in aged specimens could also result from other causes affecting optimal food intake for instance. At the calibration
696 site of Anse du Halage, a study of echinoid cohorts suggests that few individuals grow older than six years old
697 (Poulin & Féral 1994). Overall, the absence or nearly absence of growth in old invertebrate organisms makes age
698 estimates delicate to assess. In the present model, based on the combination of the ageing sub-model and other
699 mortality processes, most individuals are calibrated to die within the assumed maximum age (before 6 years old),
700 although some individuals may reach over ten years old due to the chosen stochasticity introduced in the sub-model.

701 Juveniles inside brood pouches were assumed to grow at a constant and same rate as adults but it has sometimes
702 been assumed that the brooded young may already feed and develop at a faster rate (Schatt 1985, Schatt & Féral
703 1996). At this stage, the offspring is particularly fragile and needs protection in the brood pouches to survive, which
704 prevents any monitoring of growth rates and feeding behaviours (Magniez 1983, Schatt 1985, Mespoulhé 1992).
705
706 *4.3. Ecological relevance of the IBM population model*
707
708 Upscaling the DEB-individual model to the population level in the IBM enables to simulate population structure
709 and dynamics as a response to temperature and food resource availability. In particular, the IBM enables to predict
710 the targetted effect of environmental changes on the population at the different life stages of individuals. Additional
711 environmental data would help enhance IBM reliability and improve our knowledge of populations and
712 environmental conditions in remote areas.

713 Field works are also subject to uncertainties due to the species burrowing habit which renders the assessment of
714 population structure difficult, the brittleness of specimens also limiting counting replicates (Magniez 1980,
715 Mespoulhé 1992). Important variations in population densities were noted across studies (Guille & Lasserre 1979,
716 Mespoulhé 1992, Poulin 1996, personal observations) for a same site, which may suggest either important variations
717 in population density and structure through time, which was however refuted by Poulin & Féral (1994), or important
718 biases in sampling due to the aggregative behaviour of individuals and the patchiness of distribution patterns (Poulin
719 1996).

720 The sensitivity analysis (Appendix E) showed that the model is not very much dependent on assumptions made
721 on initial population densities because the model density-dependent regulation operates through intra-specific
722 competition for food resources only. There is no agonistic behaviour among conspecific individuals as it was
723 reported in other echinoid species (e.g. *Echinometra* sp. Shulman 1990) and there is no evidence of competition for
724 space in *A. cordatus* based on field observation. Intra-specific competition in shallow-water echinoids is a common
725 phenomenon under food-limited conditions (Stevenson et al. 2015). McClanahan & Kurtis (1991) stated that in
726 *Echinometra mathaei*, when predation pressure and intra-specific competition are low, populations increase without
727 limitation and regulation operates through a decrease in food availability for individuals. The same could hold true
728 for *A. cordatus* as well.

729 Intra-specific competition for oxygen could also have a regulatory effect (Ferguson et al. 2013) since *A. cordatus*
730 shows a high oxygen consumption rate (Guille & Lasserre 1979, Magniez & Féral 1988). In muddy substrates,
731 specimens are usually observed unburied, positioned onto the sediment (instead of underneath), which was often
732 interpreted as a result of difficulties to breath inside fine sediments.

733 The sensitivity analysis also showed that the number of eggs produced by females is a controlling parameter of
734 model stability as well. There is a high variability in the number of eggs produced among females (from 9 to 106
735 eggs per female, personal communication from P. Magniez). Taking into account such a variability would introduce
736 an enhanced stochasticity in the population dynamics model if implemented and linked to each female's reproductive
737 buffer U_R and GSI values (Martin et al. 2010, e.g. for zebrafish in Beaudouin et al. 2015).

738 Finally, the model was also shown to be sensitive to background mortality (Appendix E). Although monitoring
739 mortality rates in the field is challenging, such data would greatly enhance the reliability of the IBM.

In general, the sensitivity tests showed that the model works with the current quality and quantity of data available for this species in this habitat. However, on the matter of the temporal resolution, our model needs to be expanded and further consolidated, and we consider this element as a limitation to our work in its current state (Appendix C).

4.3.1. Modelled food resources

The organic content of sediments is one of the main food resources for detritus feeders and sediment swallowers like *A. cordatus* (Snelgrove & Butman 1994) and Antarctic echinoids (Michel et al. 2016). In the present model, the organic carbon content of sediments was used as a proxy for food availability for *A. cordatus*. Intra-specific competition for food has a stronger effect on resources availability than seasonal variations in resource availability. This is in line with ecological evidences that populations of *A. cordatus* survive periods of low food resources that prevail during the austral winter. High seasonality in food resources is a common feature of polar ecosystems and species have long adapted their diet accordingly (De Ridder & Lawrence 1982, Michel et al. 2016). This has been shown in Antarctic benthic invertebrates such as shallow-water brachiopods (Peck et al 2005), cnidarians (Orejas et al. 2001), and echinoids (Brockington et al. 2001, Ingels et al. 2012). For instance, the Antarctic sea urchin *Sterechinus neumayeri* is believed to be capable of mobilizing energy from gut tissues, gonads and the body wall during the austral winter (Brockington et al. 2001), a strategy that may have been evolved in *A. cordatus* as well (Magniez 1983). Shrinking and resorption, which are sometimes hypothesized as a survival mechanism in other echinoids facing long periods of starvation, are phenomena which are still understudied (David & Néraudeau 1989, Ebert 2013) and have not been verified in *A. cordatus*. In the present model, starvation results in the redirection of the energy flow exclusively toward maintenance of structure, at the expense of other compartments. Although Magniez (1983) observed a decrease in gonadal material after the reproduction period, it is very small in females (-0.3%) and slightly bigger in males (-1.6%), and the exact cause has not been studied. It is not known whether this decrease in gonadal material can be directly attributed to a reabsorption for survival purposes or some other mechanism. The use of previously stored energy in the different compartments to sustain the maintenance of structure is assumed to be non-existent in our model. Such starvation processes could be tested in future implementation, provided sufficient data is obtained through experimental setups observing the phenomenon.

767 The two scenarios of future food availability were based on coarse IPCC and NOAA projection models for the
768 region. These simulations and associated outputs are here considered as conceivable scenarios of the influence of
769 food and temperature changes on population dynamics. They are used as a proof of concept and are by no means
770 considered as definite and reliable scenarios of population dynamics in the future. Future accurate predictions should
771 imply the integration of complex mechanisms influencing the production, transport and deposition of organic matter
772 in the ocean, the possibility of species to adapt to changing environmental conditions, and more experimental data
773 are needed to integrate the detailed influence of temperature on physiological processes. First observations suggest a
774 low response toward the applied changes in food availability, in comparison with the influence of temperature.
775 However, it cannot be concluded that the species would not be affected by future conditions in food resources in the
776 area.
777
778 *4.3.2. Temperature resilience*
779 Important differences were obtained between population structures and densities depending on future scenarios
780 and model projections made for contrasting food resources and temperature. Most importantly, the 'resistant'
781 population model of *A. cordatus* at Anse du Halage is predicted to sustain the expected changes in temperature and
782 food resources under both future scenarios although population density is also predicted to be strongly reduced. In
783 contrast, the 'vulnerable' population model predicts population extinction after a few decades of simulation. This
784 implies that a precise evaluation of the species resilience to temperatures is needed for more robust and decisive
785 models. Moreover, Antarctic echinoids were shown to present varied responses to ocean warming depending on
786 species and life stages, with higher vulnerability to warm temperatures in juveniles than in adults (Ingels et al. 2012).
787 Such a contrast suggests that more data could help fine-tune the present model.
788
789 *4.4. Relevance of the DEB-IBM approach for Southern Ocean studies*
790
791 DEB-IBM models are being developed for various applications and research fields. They are considered a
792 powerful tool for environmental risk assessment, such as the effect of toxicity (e.g. Beaudouin et al. 2015, David et
793 al 2019, Vlaeminck et al. 2019) and the impact of environmental changes on population dynamics (e.g. Saraiva et al.
794 2014, Malishev et al. 2018, Thomas & Bacher 2018, Goedegebuure et al. 2018). They can also be used to predict the

795 behaviour of microbial systems (Jayathilake et al. 2017) or bring to light underlying mechanisms of life history
796 strategies (e.g. Gatti et al. 2017). The DEB model brings ontogenetic and phenotypic variations to the population
797 model while the IBM brings stochasticity, population dynamics (e.g. competition for food), as well as learning and
798 interaction mechanisms (DeAngelis et al. 1991, Martin et al. 2012) to complement the model. The potential of the
799 DEB-IBM approach resides in the combination of both models to predict population dynamics as a response to
800 changing environmental conditions (i.e. at the individual level in the DEB model and at population level in the IBM)

801 In the present work, the DEB-IBM was used to improve our understanding of the dynamics of *A. cordatus'*
802 populations. Applications could be further developed to address conservation issues such as the designation of
803 priority areas and the definition of management plan strategies. Vast areas of the French Southern Territories have
804 recently been placed under enhanced protection of a national nature reserve based on experts' knowledge and
805 ecoregionalisation approaches (Koubbi et al. 2010, Fabri-Ruiz et al. 2020). Most areas however could not have
806 benefited from thorough benthic field studies, and ecological models can represent interesting tools to assess the
807 relevance of defined protection areas for target species and ecosystems. Such models can be useful when drafting
808 management plan strategies for determining favored ship traffic routes or areas where human activities can be
809 implemented in coastal areas of the national nature reserve of the French Southern Territories. Dynamic population
810 models allow testing different ecological scenarios in a quite straightforward way to illustrate research designs and
811 proposals. They can provide some clues to investigate the potential effect of environmental changes on key species
812 for which conservation efforts should be directed in a short to long-term strategy (Fulton et al. 2015). Dynamic
813 models can also prove useful for adaptable conservation strategies like the designation of dynamic protected areas as
814 a consequence of changing environments and ecosystems. Finally, dynamic models could be further implemented
815 into studies of ecosystem functioning and the impact of environmental changes on the alteration of sub-Antarctic
816 ecosystems.

817

818

819 **Acknowledgements**

820 The authors would like to thank Yoann Thomas and Cédric Bacher for their valuable advice during model
821 construction, and Pierre Magniez for his contribution with data on *A. cordatus* reproduction strategies. The present
822 work is a contribution to the IPEV programme PROTEKER (No. 1044) and the French LTER Zone ATelier

Antarctique (ZATA). It is also contribution no. 39 to the vERSO project (www.versoproject.be), funded by the Belgian Science Policy Office (BELSPO, contract n°BR/132/A1/vERSO) and contribution no. 13 to the "Refugia and Ecosystem Tolerance in the Southern Ocean" project (RECTO; BR/154/A1/RECTO) funded by the Belgian Science Policy Office (BELSPO). M A-P was supported by the French Foundation for Research on Biodiversity and its partners (FRB - www.fondationbiodiversite.fr). This work was supported by a "Fonds pour la formation à la Recherche dans l'Industrie et l'Agriculture" (FRIA) and « Bourse fondation de la mer » grants to CG.

CRediT author statement: M.A-P: Conceptualization, Methodology, Writing - Original draft; C.G.: Conceptualization, Methodology, Writing - Original draft; B.D.: Supervision, Writing - Review & Editing; J.P.F.: Writing - Review & Editing; T.S.: Supervision, Writing - Review & Editing.

References

Agassiz, A., 1881. Report on the Echinoidea dredged by H.M.S. Challenger during the years 1873–1876. Report on the scientific results of the voyage of H.M.S. Challenger during the years 1873–1876, Zoology, 3, 1-321.

Améziane, N., Eléaume, M., Hemery, L., Monniot, F., Hemery, A., Hautecoeur, M., Dettai, A., 2011. Biodiversity of the Benthos off Kerguelen Islands: Overview and Perspectives, in: Duhamel, G., Welsford, D. (Eds), The Kerguelen Plateau, marine ecosystem and fisheries, Société Française d'Ichtyologie, pp. 157-167.

Arnaud, P.M., 1974. Contribution a la bionomie benthique antarctique et subantarctique. Ph. D. Dissertation, Station marine d'Endoume, Marseille.

Beaudouin, R., Goussen, B., Piccini, B., Augustine, S., Devillers, J., Brion, F., Péry, A. R., 2015. An individual-based model of zebrafish population dynamics accounting for energy dynamics. PloS one, 10(5), e0125841. doi: 10.1371/journal.pone.0125841.

Brockington, S., Clarke, A., Chapman, A., 2001. Seasonality of feeding and nutritional status during the austral winter in the antarctic sea urchin *Sterechinus neumayeri*. Marine Biology, 139, 127–138? doi:10.1007/s002270100561.

Constable, A.J., Melbourne-Thomas, J., Corney, S.P., Arrigo, K.R., Barbraud, C., Barnes, D K., Bindoff, N.L., Boyd, PW., Brandt, A., Costa, D.P. et al., 2014. Climate change and Southern Ocean ecosystems I: How changes in physical habitats directly affect marine biota. Global Change Biology, 20(10), 3004-3025. doi: 10.1111/gcb.

Convey, P., Peck, L.S., 2019. Antarctic environmental change and biological response. Science Advances, 5(11), eaaz0888. doi: 10.1126/sciadv.aaz0888

David, B., Néraudeau, D., 1989. Tubercle loss in Spatangoids (Echinodermata, Echinoides): Original skeletal structures and underlying processes. Zoomorphology, 109, 39–53. doi: 10.1007/BF00312182

David, B., Choné, T., Mooi, R., De Ridder, C., 2005. Antarctic Echinoidea. Synopses of the Antarctic benthos. Koeltz Scientific Books, Königstein: 273 pp.

David, V., Joachim, S., Tebby, C., Porcher, J.M., Beaudouin, R., 2019. Modelling population dynamics in mesocosms using an individual-based model coupled to a bioenergetics model, Ecological Modelling, 398(C), 55-66. doi:10.1016/j.ecolmodel.2019.02.008.

DeAngelis, D.L., Godbout, L., Shuter, B.J., 1991. An individual-based approach for predicting density-dependent dynamics in smallmouth bass populations. Ecological Modelling, 57, 91-115. doi: 10.1016/0304-3800(91)90056-7.

DeAngelis, D.L., Mooij, W.M., 2005. Individual-based modeling of ecological and evolutionary processes. Annual Review of Ecology, Evolution, and Systematics, 36,147-168. doi: 10.1146/annurev.ecolsys.36.102003.152644

878 Delille, D., Gadel, F., Cahet, G., 1979. La matière organique dans les dépots de l'archipel des Kerguelen.
879 Distribution spatiale et saisonnière. Oceanologica acta, 2(2), 181-193.
880
881 Delille, D., Bouvy, M., 1989. Bacterial responses to natural organic inputs in a marine subantarctic area.
882 Hydrobiologia, 182(3), 225-238. doi:10.1007/BF00007517.
883
884 De Ridder, C., Lawrence, J.M., 1982. Food and feeding mechanisms: Echinoidea, in: Jangoux, M., Mawrence, J.M.
885 (Eds), Echinoderm nutrition. A.A. Balkema Publisheres, Rotterdam, pp. 57-115.
886
887 De Ridder, C., David, B., Larrain, A., 1992. Antarctic and Subantarctic echinoids from "Marion Dufresne"
888 expeditions MD03, MD04, MD08 and from the "Polarstern" expedition Epos III. Bulletin du Muséum national
889 d'histoire naturelle. Section A, Zoologie, biologie et écologie animales, 14(2), 405-441.
890
891 Ebert, T.A., 1975. Growth and mortality of post-larval echinoids. Integrative and Comparative Biology, 15(3), 755-
892 775. doi: 10.1093/icb/15.3.755.
893
894 Ebert, T.A., 2013. growth and survival of postsettlement sea urchins, in lawrence, J.M. (Ed), Sea Urchins: Biology
895 and Ecology, pp. 83-117. Developments in Aquaculture and Fisheries Science, 38. doi: 10.1016/B978-0-12-396491-
896 5.00007-1.
897
898 Fabri-Ruiz, S., Danis, B., Navarro, N., Koubbi, P., Laffont, R., Saucède, T. 2020. Benthic Ecoregionalization based
899 on echinoid fauna of the Southern Ocean supports current proposals of Antarctic Marine Protected Areas under IPCC
900 scenarios of climate change. Global Change Biology.
901
902 Fenaux, L., Malara, G., Charra, R., 1975. Effets d'un jeûne de courte durée sur les principaux constituants
903 biochimiques de l'oursin *Arbacia lixula*. I. Stade de repos sexuel. Marine Biology, 30(3), 239-244.
904 doi:10.1007/BF00390746.
905

Féral, J.P., & Magniez, P. 1988. Relationship between rates of oxygen consumption and somatic and gonadal size in the subantarctic echinoid *Abatus cordatus* from Kerguelen. In *6th International Echinoderm Congress* (pp. 581-587).

Féral, J.P., Poulin, E., González-Wevar, C.A., Améziane, N., Guillaumot, C., Develay, E., Saucède, T., 2019. Long-term monitoring of coastal benthic habitats in the Kerguelen Islands: a legacy of decades of marine biology research. In: Welsford, D., Dell J., Duhamel G. (Eds), The Kerguelen Plateau: marine ecosystem and fisheries. Proceedings of the Second Symposium. Australian Antarctic Division, Kingston, Tasmania, Australia, pp. 383-402. ISBN: 978-1-876934-30-9, doi: 10.5281/zenodo.3249143.

Ferguson, N., White, C., Marshall, D., 2013. Competition in benthic marine invertebrates: The unrecognized role of exploitative competition for oxygen. Ecology, 94, 126-35. doi: 10.2307/23435675.

Fulton, E.A., Bax, N.J., Bustamante, R.H., Dambacher, J.M., Dichmont, C., Dunstan, P.K., Hayes, K.R., Hobday, A.J., Pitcher R., Plagányi E.E. et al., 2015. Modelling marine protected areas: insights and hurdles. Philosophical Transactions of the Royal Society B, 370, 1681. doi: 10.1098/rstb.2014.0278

Gatti, P., Petitgas, P., Huret, M., 2017. Comparing biological traits of anchovy and sardine in the Bay of Biscay: A modelling approach with the Dynamic Energy Budget, Ecological Modelling, 348, 93-109. doi: 10.1016/j.ecolmodel.2016.12.018.

Goedegebuure, M., Melbourne-Thomas, J., Corney, S.P., McMahon, C.R., Hindell, M.A., 2018. Modelling Southern Elephant Seals *Mirounga leonina* using an Individual-based Model coupled with a Dynamic Energy Budget. PloS one, 13(3), e0194950. doi: 10.1371/journal.pone.0194950.

Grimm, V., Railsback, S.F., 2005. Individual-based modeling and ecology. Princeton university press.

Grimm, V., Berger, U., DeAngelis, D.L., Polhill, J.G., Giske, J., Railsback, S.F., 2010. The ODD protocol: A review and first update. Ecological Modelling, 221, 2760-2768. doi: 10.1016/j.ecolmodel.2010.08.019

Grimm, V., Berger, U., 2016. Robustness analysis: Deconstructing computational models for ecological theory and applications. Ecological modelling, 326, 162-167. doi: 10.1016/j.ecolmodel.2015.07.018.

Guillaumot, C., Martin, A., Fabri-Ruiz, S., Eléaume, M., Saucède, T., 2016. Echinoids of the Kerguelen Plateau – occurrence data and environmental setting for past, present, and future species distribution modelling. Zookeys, 630: 1–17.

Guillaumot, C., Martin, A., Eléaume, M., & Saucède, T. 2018a. Methods for improving species distribution models in data-poor areas: example of sub-Antarctic benthic species on the Kerguelen Plateau. *Marine Ecology Progress Series*, *594*, 149-164.

Guillaumot, C., Fabri-Ruiz, S., Martin, A., Eléaume, M., Danis, B., Féral, J.P., Saucède, T., 2018b. Benthic species of the Kerguelen Plateau show contrasting distribution shifts in response to environmental changes. Ecology and evolution, 8(12), 6210-6225. doi: 10.1002/ece3.4091.

Guillaumot, C., 2019. AmP Abatus cordatus, version 2019/01/17. https://www.bio.vu.nl/thb/deb/deblab/add_my_pet/entries_web/Abatus_cordatus/Abatus_cordatus_res.html

Guille, A., Lasserre, P., 1979. Consommation d'oxygène de l'oursin *Abatus cordatus* (Verrill) et activité oxydative de son biotope aux îles Kerguelen. Mémoires du Muséum National d'Histoire Naturelle, Paris, 43, 211-219.

Gutt, J., Isla, E., Bertler, A.N., Bodeker, G.E., Bracegirdle, T.J., Cavanagh, R.D., Comisco, J.C., Convey, P., Cummings, V., De Conto, R. et al., 2018. Cross-disciplinarity in the advance of Antarctic ecosystem research. Marine genomics, 37, 1-17. doi: 10.1016/j.margen.2017.09.006.

Hibberd, T., Moore, K., 2009. Field Identification Guide to Heard Island and McDonald Islands Benthic Invertebrates, a guide for scientific observers on board fishing vessels in that area, The Department of Environment,

960 Water, Heritage, and the Arts. Australian Antarctic Division and the Fisheries Research and Development
961 Corporation, Australia, ISBN 9781876934156, pp. 158.
962
963 Ingels, J., Vanreusel, A., Brandt, A., Catarino, A.I., David, B., De Ridder, C., Dubois, P., Gooday, A.J., Martin, P.,
964 Pasotti, F., Robert, H., 2012. Possible effects of global environmental changes on Antarctic benthos: a synthesis
965 across five major taxa. Ecology and evolution, 2(2), 453–485. doi:10.1002/ece3.96
966
967 IPCC, 2014: Climate Change 2014: Synthesis Report. Contribution of Working Groups I, II and III to the Fifth
968 Assessment Report of the Intergovernmental Panel on Climate Change [Core Writing Team, R.K. Pachauri and L.A.
969 Meyer (eds.)]. IPCC, Geneva, Switzerland, 151 pp. https://www.ipcc.ch/report/ar5/syr/ Accessed November 2019
970
971 Jayathilake, P.G., Gupta, P., Li, B., Madsen, C., Oyebamiji, O., González-Cabaleiro, R., Rushton, S., Bridgens, B.,
972 Swailes, D., Allen, B. et al., 2017. A mechanistic Individual-based Model of microbial communities. PLoS One,
973 12(8), e0181965. doi: 10.1371/journal.pone.0181965.
974
975 Jusup, M., Sousa, T., Domingos, T., Labinac, V., Marn, N., Wang, Z., Klanjšček, T., 2017. Physics of metabolic
976 organization. Physics of Life Reviews, 20, 1-39. doi: 10.1016/j.plrev.2016.09.001.
977
978 Kooijman, S.A.L.M., 2010. Dynamic energy budget theory for metabolic organisation, third ed. Cambridge
979 university press.
980
981 Koubbi, P., Ozouf-Costaz, C., Goarant, A., Moteki, M., Hulley, P. A., Causse, R., Dettai, A., Duhamel, G., Pruvost,
982 P., Tavernier, E. et al., 2010. Estimating the biodiversity of the East Antarctic shelf and oceanic zone for
983 ecoregionalisation: example of the ichthyofauna of the CEAMARC (Collaborative East Antarctic Marine Census)
984 CAML surveys. Polar Science, 4(2), 115-133.
985
986 Lang, J., 1967. Contribution à l'étude sédimentologique du golfe du Morbihan: Iles Kerguelen-Terres australes et
987 antarctiques françaises. Ph. D. Dissertation, Université de Paris.

Lang, J., 1971. Contribution à l'étude sédimentologique du Golfe du Morbihan (Iles Kerguelen). Comité National Français des Recherches Antarctiques, 29.

Lawrence, J.M., Lawrence, A.L., Giese, A.C., 1966. Role of the gut as a nutrient-storage organ in the purple sea urchin (*Strongylocentrotus purpuratus*). Physiological Zoology, 39(4), 281-290.

Ledoux, J.B., Tarnowska, K., Gerard, K., Lhuillier, E., Jacquemin, B., Weydmann, A., Féral, J.P., Chenuil, A., 2012. Fine-scale spatial genetic structure in the brooding sea urchin *Abatus cordatus* suggests vulnerability of the Southern Ocean marine invertebrates facing global change. Polar Biology, 35. 611-623. doi: 10.1007/s00300-011-1106-y.

Lika, K., Kearney, M.R., Freitas, V., van der Veer, H.W., van der Meer, J., Wijsman, J.W.M., Pecquerie, L., Kooijman, S.A.L.M., 2011a. The "covariation method" for estimating the parameters of the standard Dynamic Energy Budget model I: Philosophy and approach. Journal of Sea Research, 66(4), 270-277. doi:10.1016/j.seares.2011.07.010.

Lika, K., Kearney, M.R., Kooijman, S. A. 2011b. The "covariation method" for estimating the parameters of the standard Dynamic Energy Budget model II: Properties and preliminary patterns. Journal of Sea Research, 66(4), 278-288. doi: 10.1016/j.seares.2011.09.004

Magniez, P., 1979. Modalités de l'incubation chez *Abatus cordatus* (Verrill), oursin endémique des îles Kerguelen, i*n*: Jangoux, M. (Ed), Echinoderms—present and past, Balkema Press, Rotterdam, pp 399–403.

Magniez, P., 1980. Le cycle sexuel d'*Abatus cordatus* (Echinoidea: Spatangoida): modalités d'incubation et évolution histologique et biochimique des gonades. Ph. D. Dissertation, Université Pierre et Marie Curie, Paris.

1014 Magniez, P., 1983. Reproductive cycle of the brooding echinoid *Abatus cordatus* (Echinodermata) in Kerguelen
1015 (Antarctic Ocean): changes in the organ indices, biochemical composition and caloric content of the gonads. Marine
1016 Biology, 74(1), 55-64. doi:10.1007/BF00394275
1017
1018 Magniez,P., Féral, J.P., 1988. The effect of somatic and gonadal size on the rate of oxygen consumption in the
1019 subantarctic echinoid *Abatus cordatus* (Echinodermata) from Kerguelen. Comparative Biochemistry and Physiology
1020 Part A: Physiology, 90(3), 429-434. doi: 10.1016/0300-9629(88)90214-9.
1021
1022 Malishev, M., Bull, C.M., Kearney, M.R., 2018. An individual-based model of ectotherm movement integrating
1023 metabolic and microclimatic constraints. Methods in Ecology and Evolution, 9, 472–489. doi: 10.1111/2041-
1024 210X.12909.
1025
1026 Marques, G.M., Augustine, S., Lika, K., Pecquerie, L., Domingos, T., & Kooijman, S. A., 2018. The AmP project:
1027 comparing species on the basis of dynamic energy budget parameters. PLoS computational biology, 14(5),
1028 e1006100.
1029
1030 Martin, B.T., Zimmer, E.I., Grimm, V., Jager, T., 2010. DEB-IBM User Manual: Dynamic Energy Budget theory
1031 meets individual-based modelling: a generic and accessible implementation. Available at
1032 https://www.bio.vu.nl/thb/deb/deblab/debibm/DEB_IBM_manual.pdf.
1033
1034 Martin, B.T., Zimmer, E.I., Grimm, V., Jager, T., 2012. Dynamic Energy Budget theory meets individual-based
1035 modelling: a generic and accessible implementation. Methods in Ecology and Evolution, 3, 445-449. doi:
1036 10.1111/j.2041-210X.2011.00168.x.
1037
1038 McClanahan, T., Kurtis, J.D., 1991. Population regulation of the rock-boring sea urchin *Echinometra mathaei* (de
1039 Blainville). Journal of Experimental Marine Biology and Ecology, 147, 121-146. doi: 10.1016/0022-0981(91)90041-
1040 T.
1041

1042 Mespoulhé, P., 1992. Morphologie d'un échinide irrégulier subantarctique de l'archipel des Kerguelen: ontogenèse,
1043 dimorphisme sexuel et variabilité. Ph. D. Dissertation, Université de Bourgogne, Dijon.
1044
1045 Michel, L., David, B., Dubois, P., Lepoint, G., De Ridder, C., 2016. Trophic plasticity of Antarctic echinoids under
1046 contrasted environmental conditions. Polar Biology. 39, 913-923. doi: 10.1007/s00300-015-1873-y.
1047
1048 Murphy, E. and Hofmann, E., 2012. End-to-end in Southern Ocean ecosystems. Current Opinion in Environmental
1049 Sustainability, 4, 264–271. doi: 10.1016/j.cosust.2012.05.005.
1050
1051 Orejas, C., Gili, J., López-González, P.J., Arntz, W., 2001. Feeding strategies and diet composition of four Antarctic
1052 cnidarian species. Polar Biology, 24, 620–627. doi:10.1007/s003000100272.
1053
1054 Peck, L.S., Barnes, D.K.A., Willmott, J., 2005. Responses to extreme seasonality in food supply: diet plasticity in
1055 Antarctic brachiopods. Marine Biology, 147(2), 453–463. doi:10.1007/s00227-005-1591-z.
1056
1057 Poulin, E., Féral, J.P., 1994. The fiction and the facts of Antarctic brood protecting: population genetics and
1058 evolution of schizasterid echinoids, in: David, B., Guille, A., Féral, J.P., Roux, M. (Eds), Echinoderms through Time,
1059 A.A.Balkema Publishers, Rotterdam, pp. 837-843.
1060
1061 Poulin, E., Féral, J.P., 1995. Pattern of spatial distribution of a brood-protecting schizasterid echinoid, *Abatus*
1062 *cordatus*, endemic to the Kerguelen Islands. Marine Ecology Progress Series, 118, 179-186. doi:
1063 10.3354/meps118179
1064
1065 Poulin, E., 1996. Signification adaptative et conséquences évolutives de l'incubation chez un invertébré marin
1066 benthique subantarctique, *Abatus cordatus* (Verrill, 1876) (Echinodermata: Spatangoida). Ph. D. Dissertation,
1067 Université Montpellier II, Montpellier.
1068

1069 Poulin, E., Féral, J.P., 1998 Genetic structure of the brooding sea urchin Abatus cordatus, an endemic of the
1070 subantarctic Kerguelen Island. Echinoderms: San Francisco, Mooi & Telford (Eds) © 1998 Balkema, Rotterdam,
1071 ISBN 90 5410 929 7.
1072
1073 Railsback, S.F., Grimm, V., 2019. Agent-based and Individual-based Modeling: A Practical Introduction. Princeton
1074 university press.
1075
1076 Saraiva, S., Van der Meer, J., Kooijman, S.A.L.M., Ruardij, P., 2014. Bivalves: from individual to population
1077 modelling. Journal of sea research, 94, 71-83. doi: 10.1016/j.seares.2014.06.004.
1078
1079 Saucède, T., 2020. Proteker 8 cruise report. Summer campaign 2019-2020. 7th Nov. 2019 - 3rd Jan. 2020. 39 pp. [in
1080 French]. http://www.proteker.net/Campagne-d-ete-2019.html?lang=en
1081
1082 Schatt, P., 1985. Développement et croissance embryonnaire de l'oursin incubant *Abatus cordatus* (Echinoidea:
1083 Spatangoida). Ph. D. Dissertation, Université Pierre et Marie Curie, Paris.
1084
1085 Schatt, P., Féral, J.P., 1991. The brooding cycle of *Abatus cordatus* (Echinodermata: Spatangoida) at Kerguelen
1086 islands. Polar Biology, 11(5), 283-292. doi:10.1007/BF00239020.
1087
1088 Schatt, P., Féral, J.P., 1996. Completely direct development of *Abatus cordatus*, a brooding schizasterid
1089 (Echinodermata: Echinoidea) from Kerguelen, with description of perigastrulation, a hypothetical new mode of
1090 gastrulation. The Biological Bulletin, 190, 24-44. doi: 10.2307/1542673.
1091
1092 Shulman, M.J., 1990. Aggression among sea urchins on Carribean coral reefs. Journal of Experimental Marine
1093 Biology and Ecology, 140(3),197-207. doi: 10.1016/0022-0981(90)90127-X.
1094
1095 Snelgrove, P.V.R.; Butman, C.A., 1994. Animal-sediment relationships revisited: cause versus effect. Oceanography
1096 and Marine Biology: An Annual Review, *32*, 111-177

Sousa, T., Domingos, T., Kooijman, S.A.L.M., 2008. From empirical patterns to theory: a formal metabolic theory of life. Philosophical Transactions of the Royal Society B: Biological Sciences, 363(1502), 2453-2464. doi: 10.1098/rstb.2007.2230

Stenni, B., Curran, M.A., Abram, N., Orsi, A., Goursaud, S., Masson-Delmotte, V., Neukom, R., Goosse, H., Divine, D., van Ommen, T. et al., 2017. Antarctic climate variability on regional and continental scales over the last 2000 years. Climate of the Past, 13, 1609-1634.

Stevenson, A., Mitchell, F., Davies, J.S., 2015. Predation has no competition: Factors influencing space and resource use by echinoids in deep-sea coral habitats, as evidenced by continuous video transects. Marine Ecology, 36(4), 1454-1467. doi: 10.1111/maec.12245.

Thomas, Y., Bacher, C., 2018. Assessing the sensitivity of bivalve populations to global warming using an individual-based modelling approach. Global Change Biology, 24(10), 4581-4597. doi: 10.1111/gcb.14402.

Turner, J., Barrand, N.E., Bracegirdle, T.J., Convey, P., Hodgson, D.A., Jarvis, M., Jenkins, A., Marshall, G., Meredith, M.P., Roscoe, H. et al., 2014. Antarctic climate change and the environment: an update. Polar Record, Cambridge University Press, 50(3), 237–259. doi: 10.1017/S0032247413000296.

Uthicke, S., Liddy, M., Nguyen, H.D., Byrne, M., 2014. Coral Reefs, 33(3), 831-845. doi: 10.1007/s00338-014-1165-y

van der Meer, J., 2006. An introduction to Dynamic Energy Budget (DEB) models with special emphasis on parameter estimation. Journal of Sea Research, 56(2), 85-102. doi:10.1016/j.seares.2006.03.001.

Vlaeminck, K., Viaene, K.P.J., Van Sprang, P., Baken, S., De Schamphelaere, K.A.C., 2019. The Use of Mechanistic Population Models in Metal Risk Assessment: Combined Effects of Copper and Food Source on *Lymnaea stagnalis* Populations. Environmental Toxicology and Chemistry, 38, 1104-1119. doi:10.1002/etc.4391.

Waller, C. L., Overall, A., Fitzcharles, E. M., Griffiths, H., 2017. First report of *Laternula elliptica* in the Antarctic intertidal zone. Polar Biology, 40, 227-230. doi:10.1007/s00300-016-1941-y

Wilensky, U., 1999. NetLogo. Center for Connected Learning and Computer-Based Modeling, Northwestern University, Evanston, IL. http://ccl.northwestern.edu/netlogo/ (accessed February 2019).

Xavier, J.C., Brandt, A., Ropert-Coudert, Y., Badhe, R., Gutt, J., Havermans, C., Jones, C., Costa, E.S., Lochte, K., Schloss, I.R., Kennicutt, M.C. II, Sutherland, W.J., 2016. Future Challenges in Southern Ocean Ecology Research. Frontiers in Marine Science, 3:94. doi: 10.3389/fmars.2016.00094.